Development of a CRISPR-Cas13d delivery method for an antiviral strategy to interfere with the SARS-CoV-2 replication in cells

Pau Cunillera Bori

TREBALL FINAL DE GRAU BIOTECNOLOGIA

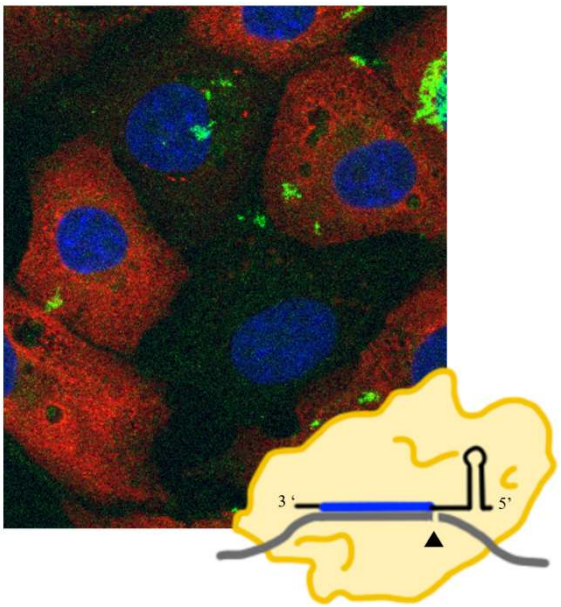

Academic tutor: Ximena Terra, Serra Húnter Lecturer, Department of Biochemistry and Biotechnology (DBB-URV), ximena.terra@urv.cat.

In cooperation with: National Center for Biotechnology - Spanish National Research Council (CNB-CSIC).

Supervisor / s: Almudena Fernández (CIBER-ISCIII) and Lluís Montoliu (CNB-CSIC), Research Scientists, Departament of Molecular and Cellular Biology, afernandez@cnb.csic.es, montoliu@cnb.csic.es.

June 2021

Jo, Pau Cunillera Bori , amb DNI 78099589F, sóc coneixedor de la guia de prevenció del plagi a la URV Prevenció, detecció i tractament del plagi en la docència: guia per a estudiants (aprovada el juliol 2017) (http://www.urv.cat/ca/vidacampus/serveis/crai/que-us-oferim/formacio-competencies-nuclears/plagi/) i afirmo que aquet TFG no constitueixen cap de les conductes considerades com a plagi per la URV.

Tarragona, 4 de juny de 2021.

Pau Cunillera Bori

A totes aquelles persones que han patit i lluitat en primera persona la COVID-19. Només la ciència ens salvarà d'aquesta, i futures pandèmies.

Als meus pares que m'han ajudat a arribar fins aquí.

INDEX

CENTER DETAILS

The present investigation has been carried out at the National Centre for Biotechnology - Spanish National Research Council (CNB-CSIC) in the Laboratory of Dr. Lluís Montoliu (*http://wwwuser.cnb.csic.es/~montoliu/indexe.html*). The study is included within the COVID-19-CSIC Project entitled "Coronavirus RNA genome destruction by CRISPR-Cas13d" led by a multidisciplinary team formed by the following researchers: Dolores Rodríguez Aguirre (CNB-CSIC), Lluís Montoliu José (CNB-CSIC) and Almudena Fernández López (CIBER-ISCIII), all of them in Madrid, and Miguel Ángel Moreno Mateos (UPO-CABD-CSIC) in Sevilla. The aim of this project is to study the ability of RNase CRISPR-Cas13d of digesting the RNA virus genome in infected mammalian cell cultures. The final aim of this proposal is to adapt it as an anti-COVID-19 drug to treat infected patients.

This work has been supervised by Lluís Montoliu and Almudena Fernández, both main researchers from their laboratory. The experiments and results presented here are limited by the schedule of the Work Placement Bachelor's Degree Subject.

ABSTRACT

The coronavirus disease 2019 (COVID-19), caused by the SARS-CoV-2 virus, pandemic has imposed an important load on global health and global economy. Preventive measures and improved treatments could help, also to broadly combat other coronavirus that may arise in the future. The described ability of SARS-CoV-2 virus to mutate and evade the current treatments highlights the need for flexible pan-coronavirus antiviral approaches. Here, we present and review the revolutionary CRISPR-Cas13d technology as a therapeutic drug for viral inhibition, emphasising its delivery challenges and avoiding a transgenic expression of CRISPR reagents. We designed and screened CRISPR RNAs (crRNAs) targeting the conserved regions of BEV equine torovirus, HcoV-229E and SARS-CoV-2 coronavirus genomes, showing the differences of their *in vitro* and *in vivo* validation. Different delivery methods of Cas13d nuclease were assessed in virus susceptible cells cultures. We found out that electroporation protein delivery is too detrimental for cell viability, suggesting the nucleic acids (DNA or RNA) transfection as a possible alternative method. Electroporation approach showed an apparently interference in SARS-CoV-2 replication in infected Vero E6 cells. Finally, we propose some improvement points to establish future CRISPR-Cas13d anti-SARS-CoV-2 strategies.

Keywords: CRISPR, Cas13d delivery, targeting, RNA virus, SARS-CoV-2.

1. INTRODUCTION

1.1 The COVID-19 pandemic

The International Committee on Taxonomy of Viruses (ICTV) has recognised 214 human RNA virus species as on July 2017, classified into 55 genera and 22 families. The yellow fever virus was the first one categorised, in 1901. RNA viruses cause an assortment of human diseases, from the common cold to life-threatening haemorrhagic fevers, and comprise viruses such as *coronaviridae* family human-infective species, HIV, dengue virus, ebolavirus and norovirus. These viruses impose an important load on global health and the global economy, as the currently pandemic has shown. Current drug development focuses on small molecules and neutralizing antibodies, which require large doses or frequent re-administration to obtain functional results (Blanchard et al., 2021; Zhang et al., 2020). Consequently, it is crucial to develop flexible, broad spectrum and effective antivirals across manifold viral species or strains. Not only treatment development is necessary to avoid future pandemics, but to take preventive measures as well. For instance, building modelling analysis by recording the spatiotemporal patterns of human RNA virus discovery results in the identification of the variables of the world most likely increasing

surveillance and diversity of their viromes (Zhang et al., 2020). This could be helpful in monitoring and avoiding future RNA virus emergencies causing health crisis.

The World Health Organization (WHO) declared, on January 30, 2020, the state of emergency and epidemic of novel coronavirus disease 2019 (COVID-19), which is caused by severe acute respiratory syndrome coronavirus 2 (SARS-CoV-2), and changed the status to pandemic on March 11, 2020 (Khodavirdipour et al., 2021). Until May 30, 2021, over 170 million global cases and more than 3.5 million global deaths have been confirmed. In Spain, over 3.6 million cases and over 79 thousand deaths have been registered (WHO Coronavirus [COVID-19] Dashboard: *https://covid19.who.int/*). To date, no cure has been reported for COVID-19 but numerous potential medicines are under clinical studies. Several treatments are being used, for instance, anti-SARS-CoV-2 monoclonal antibodies therapies or drugs such as remdesivir (nucleotide analogue drug) depending on patient disease severity (Baraniuk, 2021). Some vaccines, based on mRNA, inactivated virus vaccines or vector-based vaccines have been approved for emergency use in various countries. However, due to vaccination logistics and supply-chain problems, both pandemic numbers are still growing. Such a worldwide threat requires a deft and targeted protection strategy, which should include both preventives and treatment drugs. The appearance of other coronavirus such as severe acute respiratory syndrome (SARS) and Middle East respiratory syndrome (MERS) exhibited the potentiality of zoonotic virus emergence and increased the need to develop methods to broadly combat other coronavirus that may arise in the future (Abbott et al., 2020). Also, other four coronavirus strains are known to cause milder symptoms of the common cold (Corman et al., 2018). The analysis of the COVID-19 RNA genome obtained from confirmed patients from China, Australia, and the United States showed that the viral genome has single nucleotide polymorphism (SNPs) mutations. This ability to mutate could lead SARS-CoV-2 to evade current therapeutics approaches, further highlighting the need for a pan-coronavirus targeting strategy (Khodavirdipour et al., 2021).

1.2 *Nidovirales* genome organization

SARS-CoV-2, the Human Coronavirus 229E (HcoV-229E) (both belonging to order *Nidovirales,* family *Coronaviridae,* genus *betacoronavirus* or *alphacoronavirus* respectively, subfamily *Coronavirinae*) and the Equine Torovirus (BEV) (of the order *Nidovirales,* family *Tobaniviridae,* genus *Torovirus,* subfamily *Torovirinae*; but, historically, it belonged to the family *Coronaviridae)* possess a very similar genome organization (Kim et al., 2020; Ujike & Taguchi, 2021). Thus, these three related viruses present some common issues. Firstly, they are enveloped virus with a linear, non-segmented, positive-sense single-stranded RNA genome of ~30 kb. Its genomic RNA is translated to produce non-structural proteins (NSPs) from two open reading frames (*ORF*s), *ORF1a* and *ORF1b*, in a continued translation (figure 1). The viral

genome is also used as the template for replication and transcription, which is mediated by one of this NSP harbouring RNA-dependent RNA polymerase (RdRp) activity. The subgenomic RNAs (sgRNAs) encode structural proteins (and other accessory proteins). Their replication and transcription are located in cellular cytoplasm (Kim et al., 2020). These similarities between different coronaviruses allow the design of a commune antiviral strategy. Therefore, its validation in the three viruses could highlight its pan-coronavirus capacity. Moreover, experimental infections with HcoV-229E and BEV can be regularly done within a Biological Safety Level 2 (BSL-2) laboratory. Whereas SARS-CoV-2 infections must be carried out by specialized staff in a Biological Safety Level 3 (BSL-3) laboratory, hence complicating its manipulation. Nonetheless, we should keep in mind that their genome sequences (and the corresponding therapeutic strategies) will not have to be identical.

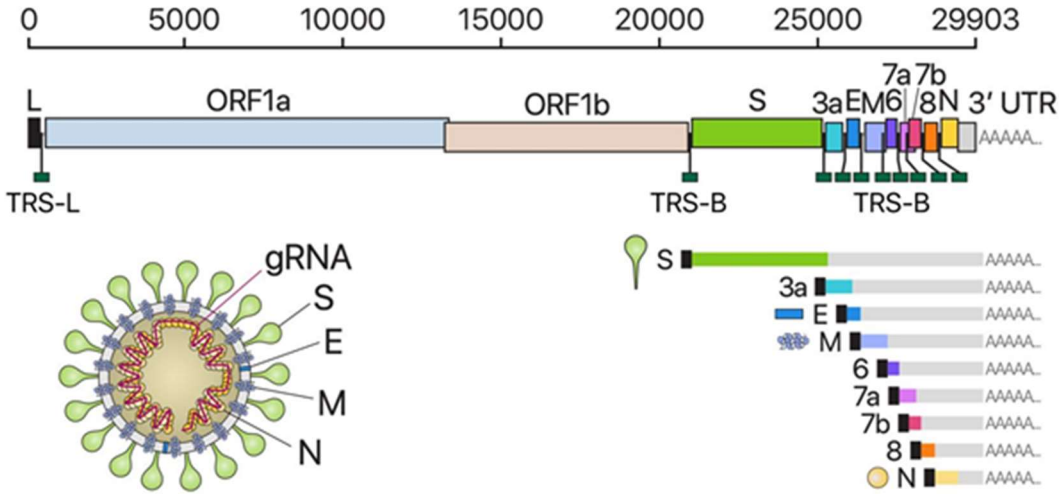

FIGURE 1 | The SARS-CoV-2 Genome Organization, Canonical Subgenomic mRNAs, and Virion Structure are depicted in a diagram. As an example of *Nidovirales* genome organization. *ORF1a* and *ORF1b* are translated from full-length genomic RNA (29,903 nt), which also acts as an mRNA. There are nine major subgenomic RNAs generated in addition to the genomic RNA. For better visualization, the boxes representing small accessory proteins are larger than the actual size of the *ORF*. The leader sequence is shown by the black box (Kim et al., 2020).

1.3 Endonucleases in gene editing technology

The short history of genome-editing approaches comprises the previously characterized nucleases; meganucleases, zinc-finger nucleases (ZFN) and transcription activator-like effector nucleases (TALEN); and the disruptive and newly discovered CRISPR-Cas technology. All of them share the same mechanism by which a gene sequence is edited. Either it can be disrupted or it can be exchanged by exogenous donor DNA molecules *via* homologous recombination (HR). Briefly, a double-strand break (DSB) at a chosen specific genomic location is produced by one of the mentioned nucleases. Then, the endogenous cellular mechanisms repair it by non-homologous end joining (NHEJ) or homology-driven repair (HDR) depending on the absence or presence of adequate donor DNA molecule with homologous sequences surrounding the DSB, respectively.

Gene-editing events are associated with HDR pathway whereas disruption events with NHEJ (supplementary figure 1) (Fernández et al., 2017).

1.4 CRISPR-Cas systems

Clustered regularly interspaced short palindromic repeats (CRISPR) and CRISPR-associated protein (Cas) are the ultimate tools available in genome-editing technologies. They have been demonstrated as powerful nucleases for editing DNA or disrupt RNA sequences and genetic information expression, with high efficiency and specificity. These genome-engineering tools have revolutionized the life sciences and they are recognized for its potentially transformative applications in biotechnology, agriculture, and medicine. CRISPR-Cas genome-editing systems are derived from elements of an adaptive immune system against environmental mobile genetic elements (MGEs), discovered and characterized in prokaryotes over two decades ago. CRISPR-Cas systems consists of three parts: the effector protein module, the acquisition module and the CRISPR array (Mojica & Montoliu, 2016; Fernández et al., 2017; Hille et al., 2018; Yan et al., 2019; Tong et al., 2021).

The biotechnological use of this microbial immune system relies on the effector protein module, such as the enzyme Cas9. It is a RNA guided sequence-dependent recognition DNase enzyme based on the principles of Watson-Crick base pairing. This results in a target DNA sequence – guide RNA (gRNA) duplex, producing a DSB. The gRNA is the synthetic form of CRISPR RNA (crRNA), targeting the desired genetic sequence, fused with a trans-activating crRNA (tracrRNA), which associates with the nuclease protein. Cas9 effector protein is derived from *Streptococcus pyogenes,* and its DNase activity is dependent on the recognition of a short sequence, called the protospacer adjacent motif (PAM), immediately upstream of the target DNA region (Doudna & Charpentier, 2014; Lander, 2016; Fernández et al., 2017; Nuñez et al., 2021). CRISPR-Cas9 has been used, for example, in the generation of permanent gene knock-out organisms or transgenic ones which can be used in the study of rare diseases, such as albinism, or mammalian genome organization (Seruggia et al., 2015, 2020; Fernández et al., 2021). Also non-catalytic Cas9 forms (dCas9) fusion proteins have been used in altering the genetic information expression and epigenetics marks, resulting in a programmable epigenetic memory writer, known as CRISPRoff, which establishes DNA repressive DNA methylation and histone modifications in a desired region (Nuñez et al., 2021).

The novel characterization of Cas12 and Cas13 effector protein families have brought new applications and opportunities. CRISPR-Cas12 systems, first derived from human pathogenic bacterium *Francisella tularensi* and reported the Cas12a effector protein, have turned into another valuable resource with many subtypes and diverse functions. Cas12 variants have been reported for targeting single stranded DNA (ssDNA) and double stranded DNA (dsDNA), whose DNase

activity also requires PAM motif-recognition. CRISPR-Cas12 have been proposed in applications such as genome editing, especially in organism not compatible with Cas9; transcriptional regulation based on dCas which either inhibits gene transcription, a method known as CRISPR interference; or activation it, a method known as CRISPR activation; Cas12 family can also be used in precise editing of single nucleotides. Furthermore, Nucleic Acid Detection Platforms have been proposed based on Cas12 effectors protein DNase activity in both *cis*- and *trans*-activity on ssDNA. In addition, Cas12g has similar function as Cas13, a RNase activity, presenting Cas12g better thermal stability and smaller size than the Cas13 nucleases. Advantageous characteristics of Cas12g which can be used in a portable *in vitro* RNA detection kit (Tong et al., 2021).

Now, CRISPR-Cas systems are the most popular genomic-editing tool due to its plasticity, simplicity and ease of use in almost every molecular biology laboratory. Many applications, which seem to be unlimited, have been proposed for engineered CRISPR-Cas system, during the last 10 years (Fernández et al., 2017; Tong et al., 2021; Piergentili et al., 2021). The present document will focus on the novel characterized Cas13d effector protein which is capable of pairing and targeting specific RNA sequence, instead of DNA as Cas9 or Cas12.

1.5 CRISPR-Cas13 as a RNA-targeting platform

In contrast to DNA editing and disruption, mapping of transcriptome changes and RNA "Knock-down" strategies have become important and advantageous in studying the cellular function and disease. Interfering with the function of individual transcript dynamics could lead to set up causal linkages between observed transcriptional changes and cellular phenotypes. Actually, upon lowering but not completely removing gene activity, it could lead to uncover phenotypes which may otherwise remain hidden due to loss-of-function lethality. Directly disrupting gene activity at the RNA level avoids the need for DNA permanent mutagenesis and subsequent laborious multi-generation genotype screening to obtain homozygous strains. Current RNA interference (RNAi) and morpholinos (MOs) technologies have failed in establishing an efficient approach without off-target effects and several challenges remain to be fixed. As a result, CRISPR-Cas13 RNA endonucleases systems become an encouraging strategy for mentioned goals (Konermann et al., 2018; Kushawah et al., 2020). Finally, targeting and cleaving a RNA sequence could be used as a therapeutic approach, for example, inhibiting RNA virus genome replication (Abbott et al., 2020; Blanchard et al., 2021).

Cas13 is a class 2/type VI CRISPR-Cas RNA endonuclease, which in the activated state, Cas13 acts as a RNase, indiscriminately cutting any exposed RNA, including target RNA, resulting in the global degradation of RNA (Hille et al., 2018). Class 2 systems possess a single multi-domain effector protein architecture, whereas a complex of multiple Cas proteins is found in class 1 systems. Class 2 systems, due to its relative simplicity, are used as a toolkit for genome

editing and other applications. Within Class 2 systems, three distinct types could be found, II (CRISPR-Cas9), V (CRISPR-Cas12) and VI (CRISPR-Cas13), which are assorted into 11 subtypes. Homologous nuclease domains are shared among class 2 CRISPR-Cas systems; specifically RuvC family DNase domain in type II and V, and HEPN RNase domain in type VI, obviously, showing low sequence conservation and substantial functional diversity. Type VI CRISPR-Cas systems are known to be capable of targeting RNA, derived from immune systems in prokaryotes (Yan et al., 2019). Previously characterized in detail, Cas13a and Cas13b type VI effector proteins present crRNA-dependent target cleavage activity and a non-specific, collateral RNase activity which is stimulated by target recognition and cleavage, both mediated by two HEPN domain contained in Cas protein. Moreover, these Cas13 proteins possess the ability to selfcatalyse the processing of the pre-crRNA into their mature form independent of divalent cations. Cas13b is considered a more robust nuclease than Cas13a. Both Cas13 type VI effector proteins can be engineered for mammalian cell RNA "knock-down" and binding. The gRNA in Cas13 systems is equivalent to crRNA because the tracrRNA is no present in their original bacterial systems (Abudayyeh et al., 2017; Yan et al., 2019).

The novel Type VI CRISPR-Cas13d (subtype VI-D) have been identified by bioinformatic mining of prokaryotic genome and metagenome and characterized in *Escherichia coli* mutants. Cas13d effector proteins show a smaller size (average length of 930 aa) than previously described Cas13a (1,250 aa) and Cas13b (1,250 aa), becoming suitable for *in vivo* delivery packaging, for example, Cas13d paired with a CRISPR array encoding multiple gRNA in versatile adeno-associated virus (AAV) delivery vehicle. No appreciable dependence on a protospacer flanking sequence (PFS) has been reported for Cas13d RNase activity (Konermann et al., 2018; Yan et al., 2019).

Firstly, Cas13d is capable of processing pre-crRNA into mature gRNA via a HEPN domain-independent mechanism. Unlike Cas13a and Cas13b, pre-crRNA processing activity of Cas13d depends on divalent cations. In addition, Cas13d lacks a counterpart to the domain considered responsible for processing in Cas13a, showing low sequence conservation among the Cas13 family and a substantial structural flexibility. These findings suggested a different biochemically mechanism of crRNA maturation in Cas13d, which generates different intermediate forms of pre-crRNA (supplementary figure 2). Mature crRNA presents a 5' direct repeat truncated by 6 nt and a spacer length between 20 to 30 nt. Secondly, guide sequence-dependent recognition of target RNA triggering HEPN-mediated RNase activity, resulting in the cleave of desired ssRNA (figure 2) and collateral RNase activity *in vitro*. Cas13d targeting is HEPN- and Mg^{2+}-dependent (Konermann et al., 2018; Yan et al., 2019).

The WYL-domain containing accessory proteins in VI-D CRISPR-Cas systems has shown the ability to stimulate Cas13d effector activity in both targeting RNA and modulating nuclease

activity (Yan et al., 2019). The maximal activity for Cas13d was reported into 24-41 ºC temperature range, suggesting activity into eukaryotic hosts. Cas13d can be engineered and attached with NLS for programmable RNA in eukaryotic context with no off-target effects detected. HEPN-inactive Cas13d (dCas13d) can pair with target coding mRNA but not necessarily perturb protein translation. Besides, dCas showed alternative splicing effector activity in a neuronal model of frontotemporal dementia. This method showed best results compared with RNAi or DNA editing with CRISPR-Cas9 (Konermann et al., 2018).

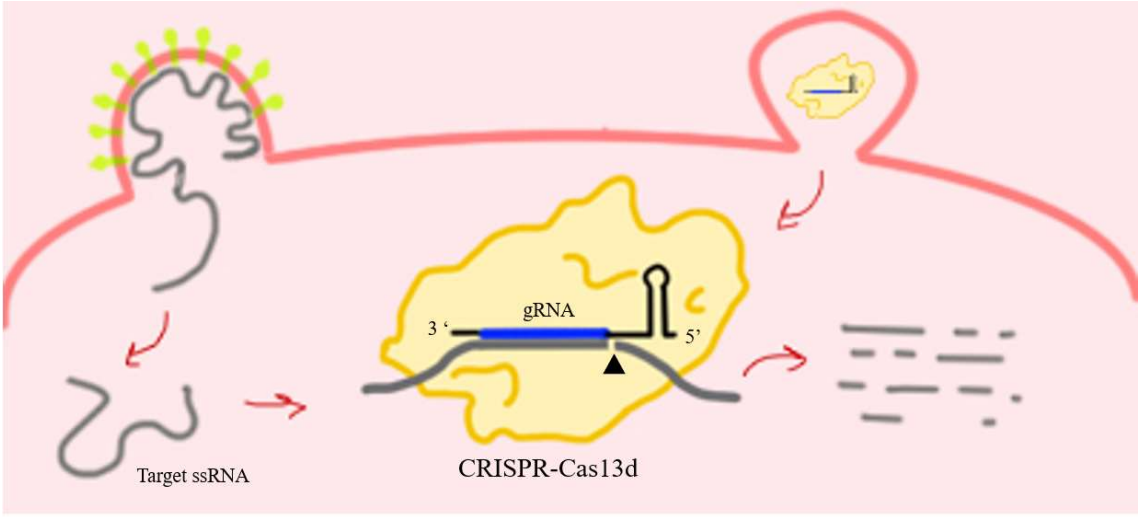

FIGURE 2 | Schematic model of CRISPR-Cas13d system showing its guide sequence-dependent recognition RNase activity on target single stranded RNA (ssRNA), resulting in RNA degradation.

1.6 Antecedents

Kushawah et al., (2020) showed that human codon optimized *Ruminococcus flavefaciens* Cas13d (*Rfx*Cas13d) in protein form or its mRNA plus gRNA provides a robust, highly efficient, specific and simple method to disrupt mRNA function in an assortment of embryonic animal models. In that study, the Cas13d technology was applied to specifically target ectopic and endogenous RNAs from relevant early developmental genes in four species of vertebrate embryos without showing off-target effects, immune reaction or stress *in vivo.* Hence, better results than the current RNAi approach, which remains ineffective, were obtained.

In the present study, a *Rfx*Cas13d, not fused with NLS, will be used due to its small size, facilitating its *in vivo* delivery, and its robust, highly efficient and specific crRNA recognition-dependent RNase activity. Moreover, collateral activity has not been detected in Cas13d nuclease in eukaryotic cellular models (Konermann et al., 2018) nor in *in vivo* embryonic animal models (Kushawah et al., 2020).

However, the CRISPR-based RNA modulation could present a short-live effect due to rapid crRNA degradation by endogenous RNA nucleases and regeneration of the cellular steady-state

by continuous target RNA expression. Constitutive crRNA and/or Cas13 expression could be achieved via genetic modified systems, prolonging the RNA modulation effects. These methods are less desirable for therapeutic approach such as targeting of immune checkpoints for immuno-oncology or antiviral strategies (Méndez-Mancilla et al., 2021).

In this line, some chemical RNA modifications and their placement into crRNA have been tested for *Rfx*Cas13d RNA targeting and knockdown to assess their effect in avoiding their cell clearance. Researchers have established which chemical modifications and in which region of crRNA showed better and more persistent RNA knockdowns. Three types of chemically-modified uridine nucleotides (3xU) or an inverted thymidine (invT) capping the 3' end, which did not interfere with target knockdown efficiency, have been studied. In addition, the chemical modification did not generally improve the performance of low-scoring guide designed sequences. The modification improved the crRNA stability only. Also, a phosphonothioate linkage (S) at the 3' end of the 23 nt spacer sequence of the crRNA has been reported as a improving modification on targeting the SARS-CoV-2 5' leader sequence of all subgenomic viral transcripts (Méndez-Mancilla et al., 2021).

One of the main barriers for CRISPR-Cas13d RNA engineering is the delivery of the effector protein into live systems, such as cell cultures, without their permanent genetic manipulation. This is not desirable in therapeutic approaches as in the present study. Some researchers have used genetic modified cell cultures or organisms expressing continuously Cas13d protein and/or crRNAs (Abbott et al., 2020; Buchman et al., 2020; Méndez-Mancilla et al., 2021), others have used transfections systems to introduce mRNA coding for Cas13 into the eukaryotic A549, Vero E6 or HEK 293T cell lines (Konermann et al., 2018; Blanchard et al., 2021) and some researchers have used virus-like particle (VLP) as delivery vehicles (Singsuksawat et al., 2021). Generally, these transient expression methods resulted in low yields.

Which is the current knowledge about CRISPR-Cas system applications in COVID-19 pandemic?

CRISPR-Cas detection methods of SARS-CoV-2 based on Cas12 or Cas13a effector proteins have been proposed by several researchers, leveraging their collateral nuclease activity on reporter nucleic acid molecules present in the *in vitro* reaction medium (Broughton et al., 2019; Kellner et al., 2019; Ding et al., 2020; Joung et al., 2020).

Nguyen et al., (2020) was the first proposal of therapeutical CRISPR-Cas13d against SARS-CoV-2 approach in February 2020. It consisted in an all-in-one AVV delivery of Cas13d effector with 3 crRNA targeting conserved SARS-CoV-2 genome regions. They designed 10,333 guide RNAs to specifically target 10 peptide-coding regions of the virus without human genome

homology and considering the SNP mutation found in first virus samples sequenced. However, experimental evidence were missing.

Blanchard et al., (2021) studied the use of CRISPR-Cas13a on destroying the RNA viral genome of an Influenzavirus (IAV) strain and the SARS-CoV-2 into eukaryotic cellular model and *in vivo* animal models (hACE2 genetically-modified mice and hamster). NLS fused and unfused Cas13a effector protein were tested for IAV due to it could be found into both cellular locations. Only unfused Cas13a was used for SARS-CoV-2 because it is only found in cytoplasm. They designed crRNA targeting *RdRp* and nucleocapsid (*N*) SARS-CoV-2 genome regions. No off-target effect detected *in vivo*. With all results collected, they concluded that CRISPR-Cas13a could be used *in vivo* against respiratory viruses. A single dose managed to alter the pathophysiology of the infection.

Finally, Abbott et al., (2020) published a strategy to counteract COVID-19 using CRISPR-Cas13d, named as PAC-MAN (Prophylactic Antiviral CRISPR in huMAN cells). They designed crRNA targeting *RdRp* and *N* regions of SARS-CoV-2 genome because these were the most conserved regions among 17 COVID-19 patients' sequences and aligned with SARS-CoV and MERS-CoV. Off-target in human transcriptome crRNA sequences were removed. Taken into account all results obtained; they concluded that PAC-MAN strategy displays a potentially powerful new therapeutic approach because it could reduce SARS-CoV-2 genome presence into human lung epithelial cell cultures treated with Cas13d. But this study presents a major drawback: it is based on genetically-modified human cells that are permanently expressing Cas13d transfected with plasmids expressing gRNAs. We consider that this strategy would not be applicable to patients. Therefore, that study should be considered as a just proof-of-concept antiviral strategy for robust and broadly targeting conserved viral sequences with Cas13d. In summary, to achieve PAC-MAN to be effective in patients, the challenge is how to deliver the Cas13d protein and crRNAs pool into the cell in sufficient amounts to cause significant desired genetic interference.

2. HYPOTHESIS AND OBJECTIVES

The hypothesis of this study states that Cas13d effector protein plus specifics gRNAs delivered into mammalian cell cultures, will interfere with the SARS-CoV-2 viral replication, which eventually will lead to reducing its viral load, and hence its infection.

We opted to target the polymerase (*RdRp*) and nucleocapsid (*N*) viral genome regions because they are highly conserved across different variants sequenced in each virus species. And, because they are essential for viral replication (RdRp protein) or for maintaining genome stability (N protein). Besides, the N sites, being placed at the 3' end, would allow targeting any of the

subgenomic RNAs produced by the virus (figure 1) (Abbott et al., 2020; Kim et al., 2020; Blanchard et al., 2021; Singh & Yi, 2021).

CRISPR-Cas13d could become a therapeutical antiviral drug to treat COVID-19 pandemic patients, a new available drug. Furthermore, CRISPR-Cas13d, due to its flexibility could be adapted to combat other virus which could arise in the future.

In this work, we aim to clone the crRNA genes targeting the *N* gene of BEV and the coding gene of *Rfx*Cas13d-*HA* into mammalian expression vectors. Moreover, we aim to characterize the *in vitro* activity and functionality of *Rfx*Cas13d effector protein, comparing its activity with two different crRNA and their differences between *in vivo* and *in vitro* crRNA validation. We aim to assess two Cas13d delivery method into mammalian cell models. Finally, the genetic intervention of CRISPR-Cas13d on targeting the SARS-CoV-2 genome in infected cell cultures will be assessed.

3. MATERIALS AND METHODS

3.1 Cell lines and viruses

The *Escherichia coli* One Shot™ TOP10 Electrocomp™ (Invitrogen) cells were transformed by electroporation using a Micropulser™ Electroporator (Bio-Rad) and the transformant plated on LB-Amp (1:1000)-Agar plates, which were incubated at 37ºC. Selected clones were cultured in LB-Ampicillin (1:1000) medium and incubated at 37ºC and at shaking. All work under microbiology sterile recommendations work conditions.

All mammalian cell lines were incubated at 5% CO_2, 95% of humidity and at +37ºC in BSL2 working conditions. The VeroE6 cells, MRC-5 cells, Equine Dermis cells (E. derm), Huh7 (hepatocyte-derived carcinoma cell line) cells, N2a (mouse neuroblastoma cell line) cells, HEK 293T (embryonic human kidney 293 cell line) cells and HEK 293T-hACE2 (hACE2 genetically-modified) cells were cultured in sterile-flattered 10% foetal bovine serum (FBS, Linus) in DMEN (Sigma-Aldrich) supplemented with 1% glutamine 200 mM (Sigma-Aldrich), 1% Pen/Strep. 100x (Sigma-Aldrich) and 0,2% Amphotericin B (Gibco) (250 µg/ml). All work done under aseptic conditions using a sterile hood (Telstar Bio II Advance). Cells were obtained from laboratory master bank. These cell lines were chosen for their susceptibility to the viruses used: VeroE6 are infected by SARS-CoV-2 virus, MRC-5 by HcoV-229E and BEV viruses, E. derm by BEV virus, Huh7 by HcoV-229E virus and HEK 293T-hACE2 by SARS-CoV-2 virus.

SARS-CoV-2 virus were kindly provided by the laboratory of Luís Enjuanes. All work with active SARS-CoV-2 was performed inside a certified BSL-3 laboratory by specialized staff with the approval of CNB-CSIC Biosafety and Ethics Committees.

BEV equine torovirus *N* gene coding plasmid vector was kindly provided by the laboratory of Dolores Rodríguez.

3.2 Mammalian expression vectors

To generate mammalian expression plasmid vectors carrying Cas13d and crRNA genes. These could be used as a template for IVT or for cell culture transfection.

The transcription of pXR003-CasRx gRNA (Addgene: #109053) results in mature CRISPR-Cas13d guide RNA (gRNA) because it possesses 5' processed DR followed by *Bbs*I sites for guide cloning. *hU6* promoter lead to transcription in mammalian cell cultures. It replicates by *pUC* ori in *Escherichia coli*.

The *CMV* promoter in pcDNA3.1 (*https://www.addgene.org/vector-database/2093/*) (modified sequence: figure 5) lead to the transcription and, subsequently, the translation to Cas13d effector protein, whose gene is cloned into pcDNA3.1 Multiple Cloning Site (*MCS*). *T7* incorporated promoter can be used for *in vitro* transcription (IVT). Replicates by *pUC* ori in *Escherichia coli.*

3.3 crRNA design and evaluation of its efficacy and Cas13d toxicity *in vivo*

In the framework of the COVID-19 project of the CSIC that concerns us, the laboratory of Dr. Miguel Ángel Moreno Mateos is in charge of designing the crRNAs for CRISPR-*Rfx*Cas13d system, targeting RNA dependent RNA polymerase (*RdRp*) and nucleocapsid (*N*) genes of the Equine torovirus (BEV), the Human coronavirus 229E (HcoV-229E) and the SARS-CoV-2 virus.

Target mRNAs were analysed *in silico* using RNAfold software (http://rna.tbi.univie.ac.at/cgi-bin/RNAWebSuite/RNAfold.cgi). *Rfx*Cas13d crRNAs are formed by 30 nt of direct repeat and 23 nt of protospacer. Protospacers of 23 nucleotides (target sequences) with high accessibility (low base-pairing probability from minimum free energy predictions) within the target mRNAs were selected to generate gRNAs. *RdRp* and *N* genes from three virus were cloned into pT3TS plasmid in order to obtain its mRNA by IVT with *T3* promoter. Then, zebrafish embryos were micro-injected with Cas13d protein (supplementary figure 3), viral *RdRp* or *N* IVT mRNA and crRNAs in order to validating the generated gRNAs efficiency, as described by Kushawah et al., (2020). Finally, RT-PCR of viral *N* and *RdRp* mRNA and a Western blot analysis of N and RdRp viral proteins, comparing 0, 2, 6 and 24 hours post infection (hpi), were carried out. *Rfx*Cas13d protein and gRNAs pools were purified and provided to us by them.

3.4 Cloning and selection of the crRNA gene targeting *N* gene of BEV

Out of the numerous crRNA tested, those named as BEV_N_gRNA6 and BEV_N_gRNA7 (supplementary table 1), were confirmed by Moreno's laboratory as having the highest activity for targeting the nucleocapsid (*N*) gene of the Equine Torovirus (BEV) (figure 3).

Chosen crRNA were ordered to Sigma-Aldrich (Merck KgaA) as a pair of DNA oligonucleotides carrying the crRNA nucleotides flanked by *Bbs*I-compatible overhangs as follows: Fw oligonucleotide (5'- AAACGG-crRNA-CT -3') and Rv oligonucleotide (5'- AAAAAG-(RC)crRNA-CC -3'). Resuspended as manufacturer recommendations. Then BEV_N_gRNA6 and BEV_N_gRNA7, in separately reactions, were cloned into pXR003-CasRx gRNA plasmid vector, and selected, by Golden Gate Cloning Method using the *Bbs*I restriction enzyme and given ampicillin resistance by the plasmid to the transformed bacteria (Engler & Marillonnet, 2011; Harms et al., 2014).

The positive clones were selected by insertion site PCR Taq DNA Polymerase Kit (Roche) and sequenced by Macrogen sequencing service. The selected positive clones were amplified in 50 ml of LB-Amp and the plasmid isolated using QIAGEN® Plasmid Midi Kit (Qiagen). Finally, NanoDrop® NB-1000 (ThermoFisher) was used for its quantification.

DNA products were visualized in 1% agarose gel electrophoresis stained with 0,003% BrEt and TBE 1x buffer, using Ready-Load® 1Kb Plus DNA Ladder (Invitrogen) and Gel Doc 2000 (Bio-Rad) with the QuantityOne software (Bio-Rad).

3.5 Cloning and selection of the Cas13d gene

The cDNA of the *Rfx*Cas13d-*HA* gene was amplified by Expand High Fidelity PCR System (Roche) protocol, because it is an above 3 kb gene, using the pT3TS plasmid vector (AddGene: #141320) (Kushawah et al., 2020) as a template. The designed pair of 30-40 bp primers used paired from 5' Kozak sequence till 3' Histidine tag gene, 2,970 bp after, flanking the whole Cas13d gene. The Fw and Rv primer were flanked by 23 nt pcDNA3.1-*Xho*I-compatible overhangs at its 5' ends (supplementary table 1).

pcDNA3.1 plasmid was linearized with *Xho*I restriction enzyme, then it was dephosphorylated with rAPid Alkaline Phosphatase (Roche) kit. Finally, it was purified using Wizard® SV Gel and PCR Clean-Up System (Promega) and quantified with NanoDrop® NB-1000 (ThermoFisher).

Cas13d gene PCR product, which included 23 nt pcDNA3.1-*Xho*I-compatible overhangs, were cloned into linearized dephosphorylated pcDNA3.1 and selected the correct plasmid with the desired insertion using the Gibson Assembly® Cloning Kit (New England BioLabs).

The positive clones were selected by insertion site PCR Taq DNA Polymerase Kit (Roche) and by restriction enzyme digestion of purified plasmid with Wizard® SV Gel and PCR Clean-Up System (Promega). The selected positive clones were amplified in 50 ml of LB-Amp and the plasmid isolated using QIAGEN® Plasmid Midi Kit (Quiagen). Finally, NanoDrop® NB-1000 (ThermoFisher) was used for its quantification.

DNA products were visualized in 1% agarose gel electrophoresis stained with 0,003% BrEt and TBE 1x buffer, using Ready-Load® 1Kb Plus DNA Ladder (Invitrogen) and Gel Doc 2000 (Bio-Rad) with the QuantityOne software (Bio-Rad).

3.6 *In vitro* RNA cleavage activity of *Rfx*Cas13d effector protein

The mRNA of *N* gene of the BEV equine torovirus was IVT using mMESSAGE mMACHINE™ T7 Transcription Kit (ThermoFisher) and the RNA purified using a NucAway™ Spin Columns (Ambion), according to manufacturer's instructions. The template was a purified *Hin*dIII-linealized pRSET-A-N (BEV), carrying the *N* gene. IVT product were confirmed via gel electrophoresis. *N* mRNA is a 500 nt sequence. It was quantified via NanoDrop® NB-1000 (ThermoFisher).

The RNA cleavage activity was assayed on mRNA obtained from *N* BEV gene. The BEV_N_gRNA2 and BEV_N_gRNA3 were tested in separately reactions at same conditions, which were added in their mature gRNA chemically synthesized forms. All the reagent preparations and additions were performed on ice. 200 ng of *Rfx*Cas13d protein and 75 ng of the crRNA (gRNA2 or 3) were mixed (unless otherwise indicated) in 2 µl Cas13d processing buffer (0.1 M HEPES, 0.75 M KCl and 2.5 mM DTT in fresh) and nuclease free water (up to a final volume 10 µl). The reaction was incubated at 37°C for 15 minutes (pre-assembling) prior to the addition of 1,000 ng of the mRNA of *N* gene of BEV (target), which one had been incubated at 75ºC for 5 min. The complete mix was incubated at 37°C for 1 hr. The reactions with only Cas13d protein, one of the gRNAs or with target mRNA alone were considered as negative controls.

For *in vitro* collateral activity assay, 200 ng of Cas9 mRNA (ThermoFisher) (as a no-target RNA for BEV_N_gRNA3) were added to the reaction buffer, following the same described protocol.

RNA products were visualized in 1% agarose gel electrophoresis stained with 0,003% BrEt and TBE 1x buffer, using Ready-Load® 1Kb Plus DNA Ladder (Invitrogen) and Gel Doc 2000 (Bio-Rad) with the QuantityOne software (Bio-Rad). Fiji/ImageJ 1.53c software was used for gel bands intensity quantifications.

3.7 Electroporation of mammalian cells

For the quantification of *Rfx*Cas13d-FAM delivery by electroporation; 400,000 cells of each cell type were resuspendended in 100 µl of Gibco™ Opti-MEM™ (ThermoFisher), then mixed with 1.6 µg of Cas13d protein and electroporated using a Gene Pulser Xcell Electroporation Systems (Bio-Rad) (100 V, 15.0 ms, 1 pulse) in its pertinent 2 mm electroporation cuvette. Subsequently, 10% FBS-DMEN only supplemented with 1% glutamine 200mM were added to final volume 500 µl. Two replicates were seeded into 24-well plate. Same method for control condition without adding Cas13d-FAM protein. All work has been carried out according to BSL2 working conditions. Cells were incubated O/N at 5% CO2, 95% of humidity and at +37ºC, before proceeding with flow cytometry analysis.

For *Rfx*Cas13d-FAM delivery prior to SARS-CoV-2 infection by electroporation; 400,000 cells of Vero E6 cell line was resuspendended in 100 µl of Gibco™ Opti-MEM™ (ThermoFisher) and mixed with the following components: 1 µg pool of SARS-CoV-2_N_gRNA3 and SARS-CoV-2_N_gRNA4 in 1:1 molar ratio, 1.6 µg of Cas13d-FAM protein or 1 µg pool of gRNAs plus 1.6 µg Cas13d protein. Then mixed with 1.6 µg of Cas13d protein and electroporated using a Gene Pulser Xcell Electroporation Systems (Bio-Rad) (100 V, 15.0 ms, 1 pulse) in its pertinent 2mm electroporation cuvette. The electroporation with only cells, pool of gRNAs or protein were considered negative controls. After the pulses, the cells were seeded at a density of 90,000-80,000 cells per well in a 24-well plate. Two replicates for each condition were seeded. On the next day cells were infected by SARS-CoV-2 virus.

3.8 Transient transfection of mammalian cell lines

The mRNA of Cas13-*HA* gene was IVT using either mMESSAGE mMACHINE™ T3 Transcription Kit (ThermoFisher) using the *Xba*I-linearized pcDNA3.1-Cas13d-HA as the template or the mMESSAGE mMACHINE™ T7 Transcription Kit (ThermoFisher) using the *Xba*I-linearized pT3TS plasmid vector (AddGene: #141320) (Kushawah et al. 2020) as a template. Both mRNAs were purified using a NucAway™ Spin Columns (Ambion), according to manufacturer's instructions. IVT products were assessed *via* gel electrophoresis. They were quantified via NanoDrop® NB-1000 (ThermoFisher).

Each cell type was plated at a density of 200,000 cells per well in a 24-well plate and transfected with either 1 µg of pcDNA3.1-Cas13d-HA plasmid vector using Lipofectamine™ 2000 (Thermo Fisher) or 1 µg of IVT mRNA coding *Rfx*Casd13d-HA protein using Lipofectamine™ MessengerMAX™ (ThermoFisher), both according to manufacturer's protocol. All work done under aseptic conditions using a sterile hood (Telstar Bio II Advance). Transfected cells were incubated at 5% CO2, 95% of humidity and at +37ºC and harvested at 24 hr or 48 hr post-transfection for their lysis and Western blot analysis. Only one replicates for each condition.

3.9 Flow cytometry

Cells which were electroporated with Cas13d protein fused with FAM fluorochrome and their controls were washed 2X in PBS and trypsinizated for 4 min at 37ºC. Then, cells were gathered in 400 µl of PBS and centrifugated at 1200 rpm and 4ºC for 3 min. The pellet obtained was resuspended in 300 µl PBS 5µM EDTA and analysed via flow cytometry (Cytomix FC-500, Beckman Coulter, USA) using the AG160075 Software Version: CXP 2.2, according to manufacturer's instructions. The confidence level was calculate using a $P < 0.05$ with n=2 and the standard deviation between the two replicates.

3.10 Western Blot analysis

Cells transfected with Cas13d-*HA* coding sequences were lysed in Laemmli´s sample buffer (62.5 mM Tris-HCl [pH 6.8], 2% sodium dodecyl sulphate (SDS), 0.01% bromophenol blue, 10% glycerol and 5% β-mercaptoethanol). Then, samples were pre-heated at 100ºC for 3 min. Protein samples were subjected to 12% SDS-polyacrylamide gel electrophoresis (PAGE) and transferred to nitrocellulose membranes (Bio-Rad). Membranes were blocked for 15 min at room temperature in Tris-buffered saline supplemented with 0.05% Tween 20 (TBS-T) containing 5% non-fat dry milk, and later incubated with primary antibodies diluted in the same buffer at 4 °C overnight. Primary antibody used in this study was mαHA H9658 (Sigma-Aldrich). Then, membranes were washed with TBS-T and incubated with goat anti-mouse IgG-peroxidase conjugate (Sigma DC02L) for 1 h at room temperature and washed again. First antibody was used at a 1:1,000 dilution in TBS-T with 5% non-fat dry milk. Second one in 1/5,000. Detection of immunoreactive proteins was carried out using the enhanced chemiluminescence (ECL) reaction (SuperSignal ThermoScientific) and detected by the ChemiDoc Touch Imaging System (Bio-Rad).

3.11 SARS-CoV-2 infection of the Vero E6 cells

The 24-well plates with seeded Vero E6 cell electroporated with Cas13d-FAM protein were infected with active COVID-19 viruses. The work was performed inside a certified BSL-3 laboratory by specialized staff with the approval of CNB-CSIC Biosafety and Ethics Committees. Established protocols for the infection, the selection of optimal multiplicity of infection (MOI), Western Blotting to detect the N protein of the virus and the plaque assays to titre the virus presence post-infection were followed.

3.12 Immunofluorescence assay viral detection

After viral infections, cells were fixed on glass coverslips for immunostaining with 4% formaldehyde for 45 min at room temperature, the overlays removed, and the cells washed three times with 1x PBS. Cells were then permeabilized with 0.5% Triton X-100 in PBS for 20 min at room temperature. Then, plates were blocked with 10% fetal calf serum (FCS) in PBS (blocking solution) for 1 h at room temperature, followed by incubation with 1/800 in blocking solution of the Rabbit monoclonal antibody (mAb) αN of SARS-CoV-2 (Genetrex, GTX 635679) fot 2 hr at room temperature in agitation. Then, plates were incubated with 1/500 in blocking solution of αrabbit Alex 549V for 1 hr at room temperature in agitation and obscurity. Viral plaques were stained with 1/200 in 1x PBS of DAPI nucleus fluorochrome for 20 min at room temperature and agitation. Finally, the coverslips were fixed on microscope sliders which were incubated O/N at room temperature in obscurity. Obtained microscope sliders were visualized using Confocal multispectral Leica TCS SP8 system and Leica DMi8 S widefield epifluorescence microscopies.

3.13 Computational designing of the primers

Primers are designed from DNA template sequence available from Addgene DataBase website (*https://www.addgene.org/*) using NCBI Primer-BLAST tool (*https://www.ncbi.nlm.nih.gov/tools/primer-blast/*). Sequences are visualized using SnapGene® Viewer 5.2.4 (GSL-Biotech). Oligonucleotides were ordered to Sigma-Aldrich (Merck KgaA) for its synthesis. All primers and gRNAs used are annotated in supplementary table 1.

4. RESULTS AND DISCUSSION

4.1 Higher depletion is found when targeting viral nucleocapsid genes

The designing of optimal crRNA is crucial for achieving a robust, highly efficient and specific crRNA recognition-dependent RNase activity in CRISPR-Cas13d. crRNA will target regions of the RNA dependent RNA polymerase (*RdRp*) and nucleocapsid (*N*) genes of model RNA virus because these are highly conserved regions and essentials for the virus life cycle. Consequently, Cas13d nuclease is used to target viral RNAs.

No potential toxicity of CRISPR-Cas13d presence into zebrafish embryos were reported by the laboratory of Dr. Moreno Mateo. Depletion is defined as the reduction in the number of copies of a determined viral sequence. According to depletion results obtained from each guide targeting each synthetic mRNA of *N* or *RdRp* gene from each *Coronaviridae* family member, it is easier to target and digest the *N* than the *RdRp* gene. In general, the resulting copy number of *N* gene detected with RT-PCR after the treatment was lower (6 hpi) (figure 3).

The crRNAs targeting the *N* gene of BEV equine torovirus (BEV_N_gRNA) 2, 6 and 7 showed a reduction of almost 90% in the number of *N* gene copies. Whereas the crRNAs targeting the *RdRp* gene of BEV equine torovirus (BEV_RdRp_gRNA) 4 and 5 showed a reduction between 60-50% (figure 3, a), which were considered no significant.

The crRNAs targeting the *N* gene of Human coronavirus 229E (229E_N_gRNA) 1 and 5 showed an efficacy of >80%. 229E_N_gRNA3 showed a 90% depletion result. The only crRNA targeting the *RdRp* gene of Human coronavirus 229E (229E_N_gRNA) with significant reduction, was 229E_RdRp_gRNA6 which showed >90% depletion score (figure 3, b).

Finally, depletion results of both crRNAs types are less efficient when targeting synthetic SARS-CoV-2 mRNA. SARS-CoV-2_N_gRNA 3 and 4 showed a reduction of 60% and 50%, respectively. Less than 50% of depletion were found when targeting *RdRp* gene of SARS-CoV-2 virus (figure 3, c). These results suggested that the design of high depletion-score gRNA for SARS-CoV-2 genome has not yet been fully achieved.

It was reported that some Cas13d orthologs presented a preference for minimal secondary structure for RNA target (Yan et al., 2019), thereby lower depletion scores were presumably associated with less accessible genome spots for the enzyme. SARS-CoV-2_N_gRNA3 binds to the same region of viral *N* gene than N3.1_*Lbu*Cas13a, N3.2_*Lbu*Cas13a (Blanchard et al., 2021) and F2-crRNA35 (Abbott et al., 2020), the best designed crRNA in previous studies, highlighting this SARS-CoV-2 virus genome spot.

The crRNAs showing ≥60% of depletion score in the zebrafish embryos test were chosen for subsequent experiments. Those crRNAs displaying <60% of depletion score were no longer considered for this project. Together these results suggested that more work has to be done to achieve better scoring-gRNAs. Specially, when targeting the *RdRp* gene.

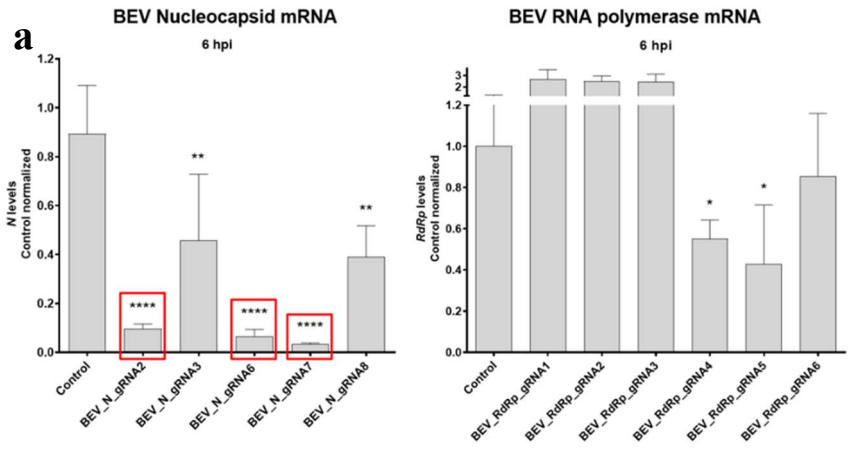

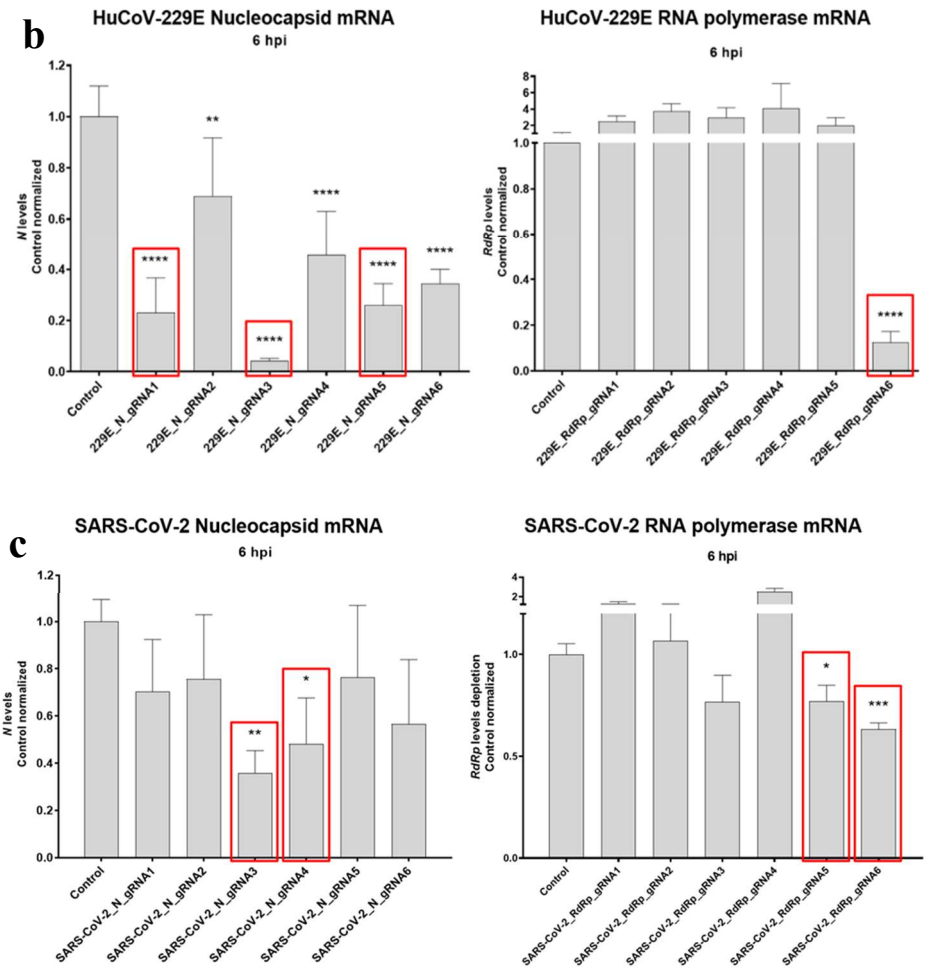

FIGURE 3 | Determination of the designed crRNA efficacy based on residual *N* gene number of copies assessed. **(a)** Results for each gRNA in comparation to controls in BEV *N* (left) and *RdRp* sequence (right) depletion. **(b)** Results for each gRNA in comparation to controls in HuCoV-229E *N* (left) and *RdRp* sequence (right) depletion. **(c)** Results for each gRNA in comparation to controls in SARS-CoV-2 *N* (left) and *RdRp* sequence (right) depletion. All figures and results graphs have been generated by Ismael Moreno from Moreno-Mateo's laboratory at CABD in Sevilla. Best considered gRNA are marked in red.

4.2 crRNA genes are cloned into mammalian expression vector

The crRNA is in charge of recognizing the target RNA sequence and binding the guide molecule to the CRSPR-Cas13d protein. The recognition of the target RNA sequences triggers the Cas13d RNase activity, leading to RNA degradation. The transcription of pXR00-CasRx plasmid carrying a crRNA gene produces mature gRNAs. The plasmid could be used into the mammalian cells transfection or in IVT. Generally, it is well-known that DNA plasmids can be easier transfected into cell cultures.

Ten pXR003-CasRx + BEV_N_gRNA6 clones and ten pXR003-CasRx + BEV_N_gRNA7 clones were randomly piked from the transformant plates to perform PCR targeting the insertion site of pXR003-CasRx using the Fw LKO primer and the Rv specific BEV_N_gRNA6 or BEV_N_gRNA7 primer (supplementary table 1). Only succesful clonings led to the analytical

~200 bp PCR product in the gel electrophoresis (figure 4, a). The plasmids isolated from the positive incubated clones were sequenced. Their *in silico* alignment product with the reference sequence pXR003-CasRx + BEV_N_gRNA6 (figure 4, b) or + BEV_N_gRNA7 (figure 4, c), respectively, showed no mutations.

Finally, a pXR003-CasRx + BEV_N_gRNA6 and a pXR003-CasRx + BEV_N_gRNA7 positive clones were amplified and the plasmid isolated, obtaining 760,5 ng/µl and 915,6 ng/µl, respectively.

All results obtained show that BEV_N_gRNA6 and BEV_N_gRNA7 were successfully cloned into pXR003-CasRx gRNA expression vector for Type VI-D CRISPR Effectors, respectively. Further research is needed to validate if transcribed gRNAs are funcional and can trigger Cas13d effector protein nuclease activity.

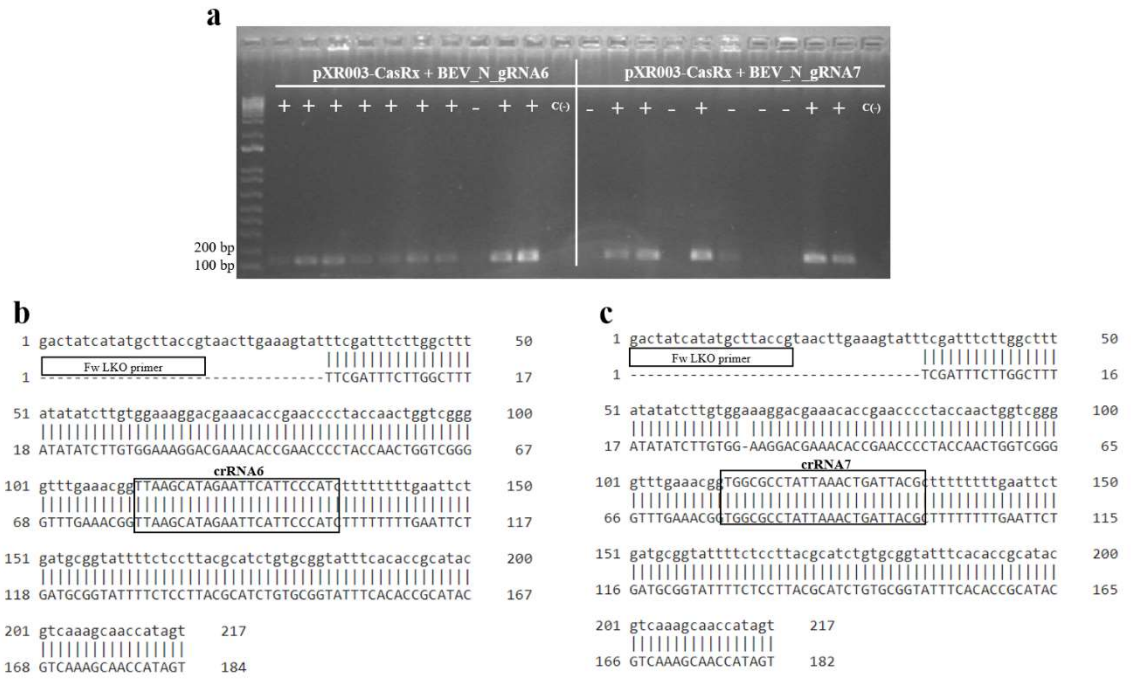

FIGURE 4 | The selection of the correct BEV_N_gRNA6 and BEV_N_gRNA7, respectively, cloned plasmid. **(a)** Visualization of above 200 bp bands from random colonies PCR, found in transformant plate, in a gel electrophoresis. The BEV_N_gRNA6 is in the left and the BEV_N_gRNA7 in the right. **(b)** The alignment between reference sequence pXR003-CasRx + BEV_N_gRNA6 (up) and the cloned crRNA6 site obtained (down). **(c)** The alignment between supposed pXR003-CasRx + BEV_N_gRNA7 (up) and the cloned crRNA7 site obtained (down).

4.3 CRISPR-Cas13d gene is cloned into a mammalian expression vector

The transcription and translation of cDNA of the *Rfx*Cas13d-*HA* cloned into pcDNA3.1 mammalian expression vector would result in Cas13d effector protein fused with a histidine tag, which can be used for protein visualization in a Western-blot method, for example. The plasmid could be used into the mammalian cells transfection or in IVT.

Twelve clones were randomly piked from the transformant plates to perform PCR targeting the insertion site of pcDNA3.1 using Fw T7 primer and a Rv Cas13d primer. Only successful cloning led to the analytical ~400 bp PCR product in the gel electrophoresis (figure 5, a). Positive clones were incubated and then they were subjected to *Pst*I digestion. The insertion of Cas13d-*HA* gene into MCS of pcDNA3.1 changes *Pst*I digestion products. If Cas13d is cloned, the digestion products are about 4,354 bp and 4,080 bp whereas 1,356 bp and 4,072 bp DNA fragments are generated in case of failed o wrong cloning, as in the original pcDNA3.1 control sample (figure 5, b). A selected digestion positive clone was sequenced and aligned with *in silico* designed pcDNA3.1-Cas13d-HA. No mutations were found in the cloned sequence (figure 5, c). Finally, it was amplified and purified at 968,3 ng/µl concentration.

All results obtained show that Cas13d-*HA* gene was successfully cloned into mammalian expression plasmid; pcDNA3.1.

Before the final successful cloning attempt, there were several unsuccessful attempts to clone Cas13d gene into the plasmid (*data not shown)*. At some point, the MCS region of the pcDNA3.1 plasmid, which was used for the failed experiments, was sequenced. The alignment between the sequence of this experimental plasmid and its sequence from internet databases did not match (figure 5, d). More than 50% mismatches were found between the overhangs. This meant that designed compatible-overhangs added to Cas13d PCR products could not match with the linealized dephosphorylated pcDNA3.1 ends. Consequently, cloning method failed.

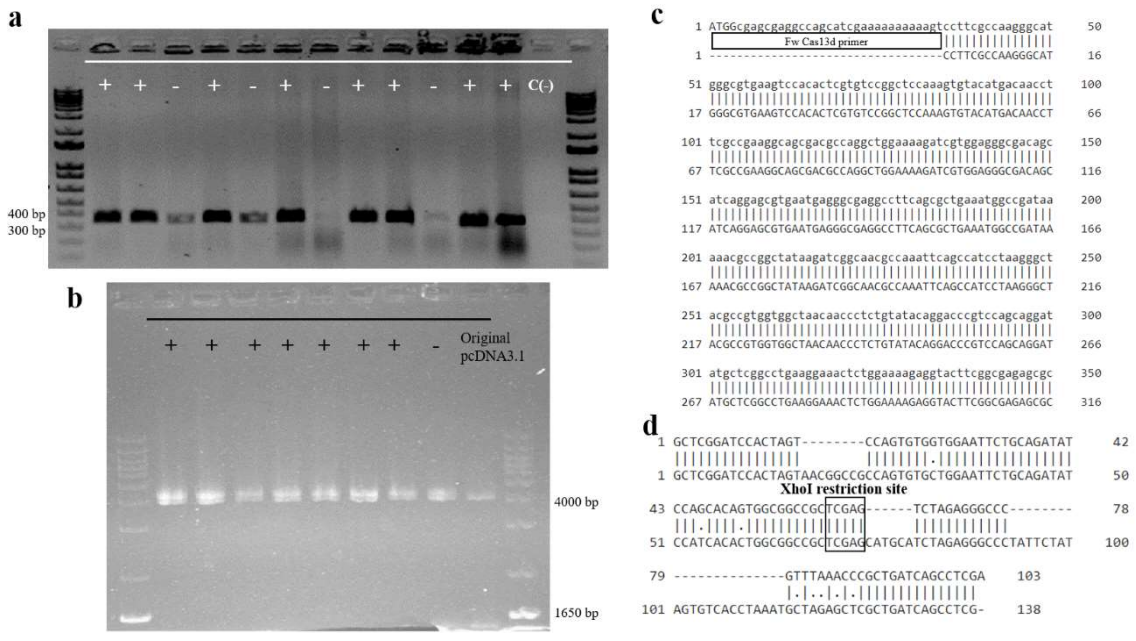

FIGURE 5 | The selection of correct Cas13d-*HA* gene plasmid cloned. **(a)** Visualization of 370 bp bands from random colonies PCR, found in transformant plate, in a gel electrophoresis. **(b)** Visualization of 4,354 bp and 4,080 bp bands of *Pst*I digestion products of cloned plasmids in a gel electrophoresis. **(c)** The first 350 nt of the gene cloned into insertion site alignment between the reference pcDNA3.1-Cas13d-HA (up) and the obtained pcDNA3.1-Cas13d-HA (down). **(d)** The alignment between MCS sequence from internet pcDNA3.1 (up) and sequenced MCS of pcDNA3.1 used in the experiment (down), showing several indels and nucleotide changes.

Subsequently, the overhangs of the Cas13d gene primers were redesigned using the confirmed pcDNA3.1 *MCS* sequence, resulting in the explained cloning success, therefore illustrating the relevance of double-checking the correct DNA sequences of vector plasmids.

These previous results showed that the homology between the 23 nt DNA fragment compatible-overhangs and flanking sequences of insertion site are important for performing a successful Gibson Assembly® Cloning Method.

4.4 *Rfx*Cas13d-FAM can cleave viral mRNA *in vitro*

Using purified *Rfx*Cas13d protein fused with FAM fluorochrome, its ability to digest the *N* gene of BEV equine torovirus was assessed *in vitro*. Two BEV_N_gRNAs were tested to characterize their differences in RNA digestion, thereby illustrating the differences between validating CRISPR reagents between an *in vivo* or *in vitro* context. The BEV *N* mRNA consists in a RNA sequence ~500 nt long.

The visualization of the IVT product of the plasmid carrying the BEV *N* gene showed two RNA bands in the gel electrophoresis. The desired mRNA was that of ~500 nt whereas the ~850 nt band was interpreted as the likely same sequence but in a secondary structure form. Also, it showed no RNA degradation (figure 6, a). The quantification of purified mRNA yielded at 1,141.3 ng/µl.

Non-lineal forms of the RNA sequence alter their migration pattern in native gels so that they will not migrate according to its true size. When the same IVT RNA product was pre-heated for 5 min at 75ºC and then assessed in a gel electrophoresis, the longer band faded away (figure 6, b). This suggested that high temperature could denature secondary structure without degrading the RNA molecule. If this was a different sequence it would not disappear, or it would show a degradation smear, so both bands could be the same sequence in different structural forms. A degraded RNA was found when it was pre-heated for 10 min (figure 6, c).

We confirmed that preassembled *Rfx*Cas13d-FAM with both gRNA, known as ribonucleoproteins (RNPs), could efficiently digest the BEV equine torovirus nucleocapsid gene transcript, showing a degradation smear in both guides plus Cas13d protein presence (figure 6, d). No RNA degradation was found for only gRNA- or Cas13d-effect. An ~850 nt and a ~500 nt were still found in the four control conditions (only gRNAs, only the nuclease protein or only the target mRNA) (figure 6, d). Although, the mRNA sample was pre-heated for 5 min at 75ºC before mixing into digestion buffer, as reported before (figure 6, b), secondary structures appeared again, probably, during subsequent Cas13d-digestion incubation at 37ºC. But both bands were digested by the RNP suggesting that they carried the same sequence (figure 6, d), with secondary structures that did not involve the crRNA-binding region, or showing CRISPR-Cas13d *in vitro* collateral

activity, as reported in previous studies (Konermann et al., 2018; Yan et al., 2019). Actually, detecting *trans* RNase activity of the enzyme was not an objective of this experiment.

In vitro cis CRISPR-Cas13 RNase activity had been described in previous studies, also concretely in *Rfx*Cas13d enzyme, where similar results were presented (Konermann et al., 2018; Yan et al., 2019; Blanchard et al., 2021; Singsuksawat et al., 2021; Méndez-Mancilla et al., 2021).

The presence of only BEV_N_gRNA 2 or 3 resulted in altered migration of both bands in both sample (figure 6, d). These results suggested that the gRNAs binds to the mRNA sequence, producing no catalytic activity on it, but clearly altering the electrophoretic mobility upon behaving as a duplex, and presumably a longer nucleic acid.

The relative intensity band in the gel after RNPs activity showed that both guides worked apparently different, following *in vitro* conditions. Firstly, the intensity rate between that of ~850 nt and that of ~500 nt band (intensity 850 nt band/500 nt band) were calculated in RNPs presence lanes and in those that only the guides and the target RNA were mixed (figure 6, d). Secondly, the resulting rate in each RNP land was normalized on the rate in its respective BEV_N_gRNA land (control) (intensity rate in RNP land/the intensity rate of respective gRNA). Finally, both resulting digestion percentages were compared. The RNP containing the BEV_N_gRNA3 digested 0.95 parts of the target RNA present in the reaction buffer, whereas the RNP using the BEV_N_gRNA2 digested 0.82 parts of RNA present in its reaction buffer.

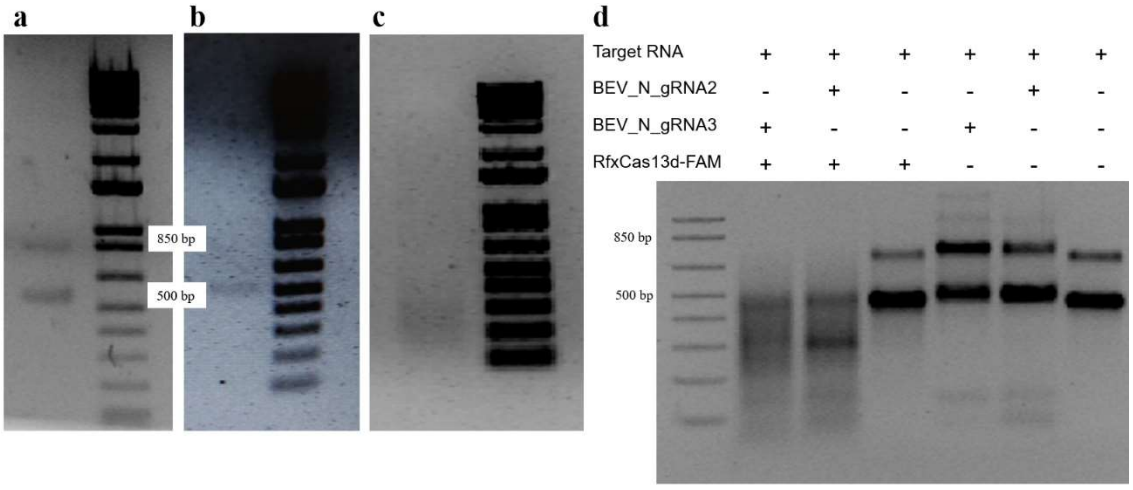

FIGURE 6 | *In vitro* RNA digestion assay of *Rfx*Cas13d. **(a)** IVT of the *N* gene of BEV assessed in a gel electrophoresis showed the target mRNA of ~500 nt and a second ~850 nt product, without RNA degradation. **(b)** Visualization of the obtained mRNA pre-heated for 5 min at 75ºC in a gel electrophoresis, showing only the desired ~500 nt mRNA. **(c)** Pre-heating the mRNA product for 10 min at 75ºC resulted in RNA degradation in a gel electrophoresis. **(d)** Gel electrophoresis showing the cleavage *in vitro* activity of the *Rfx*Cas13d protein showing smeared RNA.

The CRISPR-Cas13d crRNAs, BEV_N_gRNA2 and BEV_N_gRNA3, were reported with an above 0.9 and 0.5 points of depletion score against synthetic N gene transcript in *in vivo* zebrafish assay, respectively (figure 3, b). In contrast, Cas13d-BEV_N_gRNA3 complex

apparently digested more RNA than the complex with gRNA2, following *in vitro* conditions. A different trend was observed between *in vivo* and *in vitro* validation. These results suggested that cellular *in vivo* atmosphere affected the CRISPR-Cas13d efficiency and robustness, not only a high-scoring guide designed will result in a strong and persistent RNA knock-down. *In vivo* validation method is usually considered more robust than purely *in vitro* methods when the gRNA has to be selected for a therapeutic approach, such as presented in this document, because their subsequent RNPs are going to be tested and work in a cellular context.

The results showed that the pool of purified *Rfx*Cas13d-FAM protein available and the gRNAs pool were in good conditions and in an active/mature form, and that they did not undergo structural alterations during refrigerated transportation between collaborating centres, CABD in Sevilla and CNB in Madrid.

We next assessed collateral activity of *Rfx*Cas13d enzyme by supplementing the same reaction buffer with a ~1,650 nt unrelated RNA sequence (i.e. Cas9 encoding RNA) which was not targeted by the BEV_N_gRNA3. In figure 7, we observed as the RNP degraded the mRNA of *N* gene of BEV by the homology between it and the BEV_N_gRNA3 in similar way as reported before (figure 6). The percentage of RNA no target digested in activated RNP presence was calculated in the same way, normalizing the ~1,650 nt band intensity respect upper background intensity. Apparently, 0.2 parts of the RNA no target were digested in RNP lane respect the lane with no protein addition (figure 7). This result suggested that the CRISPR-*Rfx*Cas13d maybe possessed *trans* RNA cleavage activity *in vitro*.

The *in vitro* collateral activity of Cas13d effector protein derived from *Ruminococcus flavefaciens* was also reported in previous studies (Konermann et al., 2018; Yan et al., 2019). However, this activity type was catalogued as a moderate effect (Konermann et al., 2018). Consequently, it could be difficult to assess collateral activity in a gel electrophoresis by quantifying the intensity of RNA bands using an image-analysing software. In these previous studies, labelled RNAs sequences were used to assess *Rfx*Cas13d collateral activity, presumably with better accuracy.

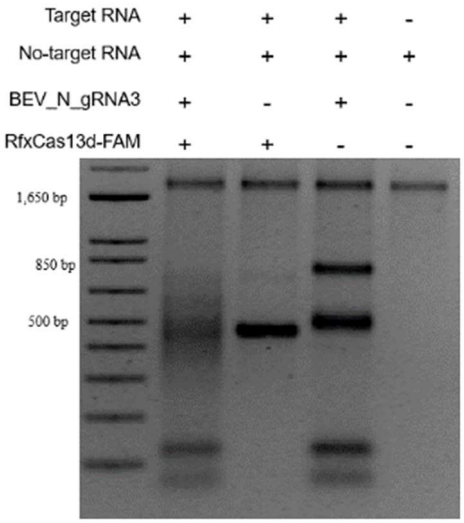

FIGURE 7 | *In vitro* RNA cleavage by *Rfx*Cas13d showing predominant on-target RNA cleavage activity on the RNA products of 500 nt and 850 nt with moderate collateral activity on 1,650 nt off-target RNA product.

4.5 Cas13d delivery into cell cultures remains challenging

We next wanted to assess which was the best delivery method for CRISPR-Cas13d reagents into cultured mammalian cells. Electroporation and DNA or RNA lipofectamine transfection methods were studied to deliver Cas13d effector protein in order to, in a subsequent experiment, test the effect of delivered RNPs on virus model infections. These methods are envisaged to overcome the necessity of carrying out genetic modified cells lines and, thus, using a more suitable experimental system for an eventual therapeutic approach.

MRC-5, Vero E6, E. derm, Huh7 and HEK 293T-hACE2 cell lines were electroporated with Cas13d protein fused with FAM fluorochrome and assessed by flow cytometry analysis. Forward and side scatters reported values showed a general tendency to mortality, and hence, a low cellular stability during the whole protocol. The figure 8 shows the forward and side scatters graphs of Vero E6 cells samples, as an example of the general tendency. Reported events have a tend to increase their side scatter, so the cellular structure complexity, and reduce their forward scatter, so cellular size. These results suggested that cells were losing their cytoplasmatic content, also the desired protein, through plasma membrane porous which were a consequence of electroporation and subsequent cells manipulation.

Results from scatterplots suggested that, the percentage of cells correctly transfected with the Cas13d-FAM signal were under 20%, for all five cellular types tested. For instance, Vero E6 cells showed an 8.62 ± 5.3% of successfully transfected cells. These yields were considered too low to perform a proof-of-concept of antiviral capacity of CRISPR-Cas13d using this delivery method. However, the delivery of Cas13d and/or crRNAs by electroporation was chosen to perform a SARS-CoV-2 infection experiment.

Flow Cytometry data obtained post-electroporation showed, in all cellular types studied, that the method was too detrimental for the cell viability. A low percentage of protein intake implies the need for a Fluorescence-activated cell sorting (FACS) approach, in order to obtain a pool of cells carrying a significant amount of the Cas3d-FAM effector protein. This procedure would lead to damaged cells which would not overcome a subsequent viral infection. Therefore, the delivery of Cas13d as a protein, remains challenging. Furthermore, no electroporation-based delivery of CRISPR-Cas13d reagents has been found in the literature

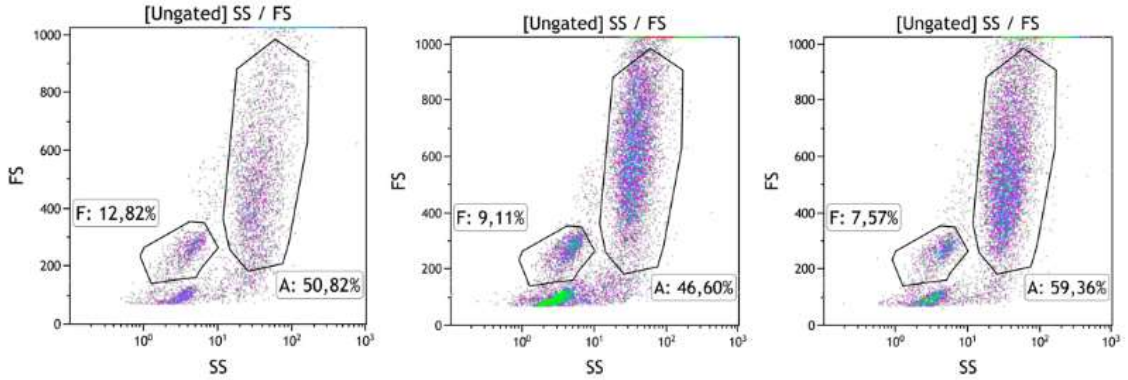

FIGURE 8 | Forward and side scatters values obtained from Vero E6 population cells electroporated with Cas13d-FAM protein showing cellular damaging indicators. Left graphs correspond to control, the two right graphs, to replicate samples.

Vero E6, Huh7, E. derm and MRC-5 cells were transfected with nucleic acids (DNA or RNA) encoding Cas13d-HA nuclease using lipofectamine carriers. Neuroblastoma N2a and HEK 293T cell lines were used as control conditions based on laboratory experience for their routine use in CRISPR-Cas9 experiments. Moreover, two types of Cas13d sequences were employed, as an IVT mRNA and as a pcDNA3.1 plasmid vector carrying Cas13d gene (figure 5). Then, we analysed Cas13d protein production by Western Blotting using the histidine tag attached to it.

As shown in figure 9, a, only positive Cas13d protein production was found in control cell lines and Vero E6 and Huh7 cells when pcDNA3.1-Cas13d-HA was used as the donor sequence. In addition, HEK 293T and Huh7 cell lines were observed to accumulate larger amounts of Cas13d protein, suggesting more protein production in these cell cultures. These results confirmed that Cas13d gene was successfully cloned into the mammalian expression plasmid vector (figure 5). Positive result in Huh7 cells suggested that this delivery method could be used in Cas13d-antiviral approach in HcoV-229E virus infection experiments. Besides, also this method could be used in SARS-CoV-2 infection in Vero E6 cells experiments.

Messenger RNA transfection resulted in no protein production in any cell type (figure 9, a). Blanchard et al., (2021) and Konermann et al., (2018) showed that mRNA had been successfully transfected in Vero E6 and HEK 293T cells cultures. Consequently, negative results in N2a, HEK 293T, Huh7 and Vero E6 cell lines suggested that our mRNA pool were degraded at the beginning of the experiment (figure 9, a).

Together these results, suggested that delivery of Cas13d reagents into E. derm and MRC-5 cells (figure 9, a) remains a challenge to be solved before testing the therapeutic approach for interfering with the BEV infection.

We next repeated the Cas13d-HA mRNA transfection of Huh7 cells comparing the delivery of mRNA *in vitro* transcripted either via mMESSAGE mMACHINE™ T3 or T7 Transcriptions Kits from two different plasmid templates. T7 Kit was used when the pcDNA3.1- Cas13d-HA plasmid (figure 5) was the template. Moreover, the presence of Cas13d-HA protein was assessed into different times of incubation, at 24 hr or at 48 hr.

The transfection of pcDNA3.1-Cas13d-HA resulted in protein production at 48 hr (figure 9, b) of incubation, recapitulating the results obtained before in Huh7 cells line (figure 9, a). Only Cas13d protein was found when cells were transfected with its mRNA obtained via T3 Kit at 24 hr of incubation.

These results showed that 24 hr of incubation after mRNA transfection were optimal for Cas13d protein production. Besides, they suggested mMESSAGE mMACHINE™ T3 was more efficient than T7 Transcription Kit because mRNA from this last kit did not induce any translation in cells. Finally, after 48 hr the Cas13d protein, which was encoded *via* mRNA, could undergo a cellular protein degradation process.

These results helped to determine the optimal time and methodology conditions for introducing CRISPR-Cas13d reagents into cell populations. Thereafter, this protocol could be used for the proof-of-concept experiments of the antiviral strategy.

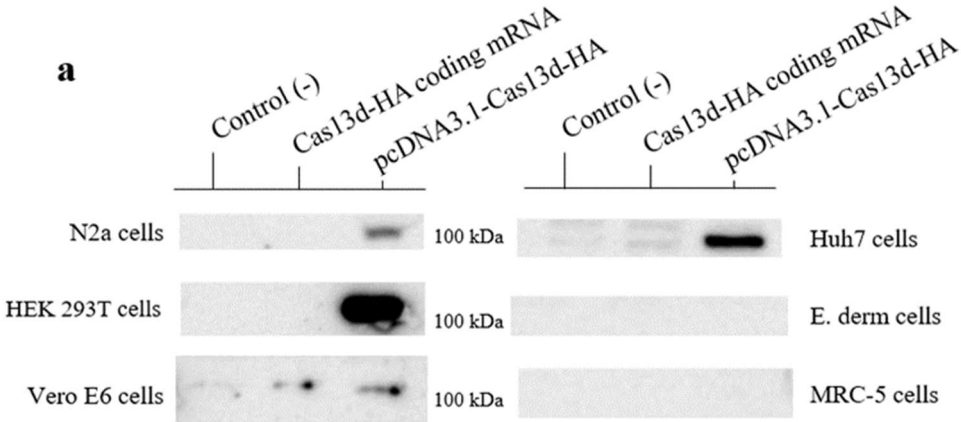

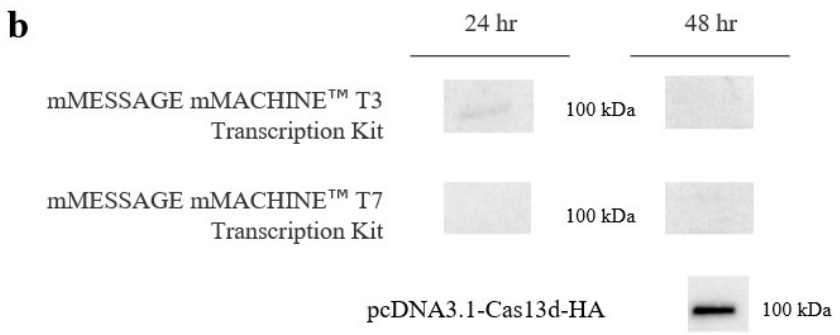

FIGURE 9 | Cas13d-HA protein purification (105 kDa) by Western Blot. **(a)** Protein detected after transfection of Cas13d coding DNA gene or mRNA in 6 types of cell lines. N2a and HEK 293T cells were used as control cell population. **(b)** Protein detected after transfecting Cas13d coding mRNA in Huh7 cells, facing two *in vitro* Transcription Kits and incubations times.

4.6 CRISPR-Cas13d apparently limited the SARS-CoV-2 viral infection

We assessed the genetic interference due to delivered Cas13d RNPs were able to carry out in SARS-CoV-2 virus-infected Vero E6 cells cultures, as a first proof-of-concept experiment of this project. The prior delivery of the drug was due to BSL-3 restrictive manipulation of infectious SAR-CoV-2 viruses. A pool of SARS-CoV-2_N_gRNA3 and SARS-CoV-2_N_gRNA4 were tested as a mix of guides in charge of driving Cas13d effector protein to bind, target and digest the *N* gene of the virus and, thus, reducing the viral genome presence into the cellular cytoplasm.

We chose both guides because they were reported as the sequences with best depletion scores when they were validated in zebrafish embryos against the viral genome plasmidic reporters (figure 3, c, left graph). SARS-CoV-2_N_gRNA 3 and 4 showed an above 0.6 and 0.5 points of depletion of *N* viral gene number of copies, respectively, in zebrafish experiments. These values were far from optimal, and thus considered the first cavea of this experiment. Furthermore, based on recent zebrafish testing experience, combining a good depletion score-gRNA, as gRNA3, and a bad-score one, as gRNA4, could result in general bad CRISPR-Cas13d performance.

Other determining factor for the efficacy of the antiviral approach is the quantity of transfected Cas13d RNPs into the cell cytoplasm. In this case, the relatively low 8.62 ± 5.3% percentage of Cas13d effectively electroporated in Vero E6 cells (figure 8) could impair finding significant differences between control and treatment conditions. In optimal conditions, more than a half of Vero E6 population cultured should have incorporated the protein and the gRNAs.

The counting of cellular concentration in each condition, before the inoculation of SARS-CoV-2 had been applied, showed population differences. A reduction of above 33% in cellular population treated with *Rfx*Cas13d-FAM alone (figure 10, a, treatment C) were reported. Whereas no significant population differences were found in the other treatments. These findings

confirmed that the delivery of Cas13d protein form by electroporation was a too detrimental procedure for the viability of the cells. Also, these suggested that maybe *Rfx*Cas13d-FAM alone was toxic for Vero E6 cells due to possibly protein aggregations may occurred.

The cells were infected with a Multiplicity of Infection (MOI) ~1 taken in consideration the number of cells presents in treatment A, B and D that was $1.8x10^5$ cells/well (figure 10, a, treatments). Consequently, in the case of cells with the C treatment that has only $1.2\ x10^5$ cells/well, the viral production will be lower in proportion with the number of cells. As shown in figure 10*,* a*,* in Cas13d RNPs sample, it was observed a slight reduction of 40% in virus titre 24 hpi, it meant that less virus particles were produced at the same time. In the case of C the viral production were normalized to $1.8x10^5$ cells/well. Although this reduction is moderate, it is statistically significant, and it suggests that possibly the CRISPRS technique could be useful. Nevertheless, this reduction was not considered as biologically significant. However, when the levels of viral N protein were analysed by Western blot no significant differences among the different conditions were observed. By Western blotting, the accumulation of N protein inside the cells were normalized respect the production of housekeeping gene of Histone H3. These results did not recapitulate viral titre tendence to decrease in the presence of RNPs.

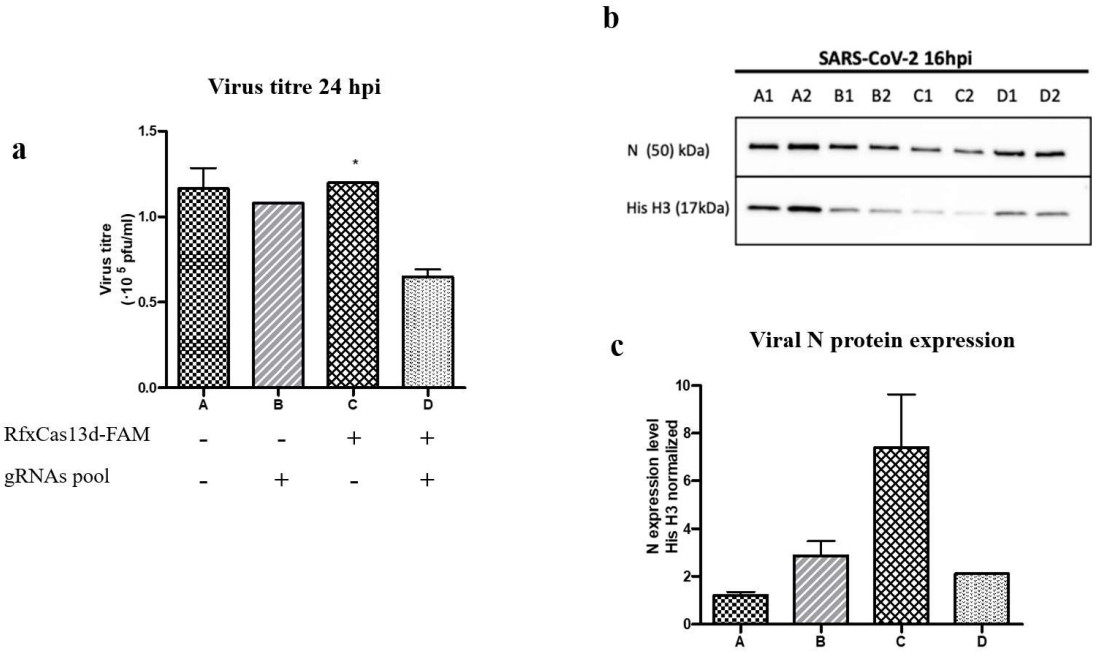

FIGURE 10 | Effect of prior administration of Cas13d RNPs on SARS-CoV-2-infected Vero E6 cells. **(a)** Treatments description and virus titre found 24 hpi. Treatment C (*) is cell number normalized. **(b)** Viral N protein and Histone H3 purification found 16 hpi in cells samples. **(c)** Quantification of N protein normalized to housekeeping protein Histone H3. All data collected and represented by Fernando Almazán from experiments done under BSL-3 working conditions. Standard deviation error bars were represented.

To see in detail the distribution of Cas13d-FAM protein electroporated into Vero E6 cells and its correlation with SARS-CoV-2 N protein distribution, the obtained microscope sliders with stained fixed cells were observed using Advanced Confocal Light Microscopy. Thus, conducting a study at individual cell level.

In all treatments, the labelled viral N proteins were stained with Alex 549V, which emitted red light in the microscopy, and showed a normal distribution throughout the cell cytoplasm during an infection (figure 11, a). The different stages of SARS-CoV-2 infection could be seen in cells because the virus life cycles were not synchronized. In treatment D and C, the analysis of green light emitted by FAM fluochrome attached to Cas13d protein showed an uneven distribution.

The general tendency for the Cas13d protein was to form protein aggregates. These appeared to be located, in general, attached to the outer part of the plasma membrane, triggering its deformation, as observed in side views of different cells obtained from several optical section in confocal imaging (figure 11, b).

Together these results suggested that these aggregates were not available for the SARS-CoV-2 RNA genome replicating in the cytoplasm, and only a few Cas13d effector protein was available as an active form throughout the cell cytoplasm to bind and digest the *N* gene of SARS-CoV-2 viruses. The low success in delivering Ca13d protein inside the cells through an electroporation method recapitulated the data observed in the flow cytometer (figure 8). Consequently, no significant and undoubtful relation could be established between a reduction in viral red fluorescence associated with the green fluorescence derived from the RNPs presence inside the cellular cytoplasm. Occasionally, individual cells were observed with this expected tendency (figure 11, c).

All results collected showed that the delivery of the Cas13d RNP is a parameter needing further optimization before we can elucidate whether the CRISPR approach is useful to reduce the viral infection. Future experiments will be performed using more efficient guides and better transfection methods of the RNPs.

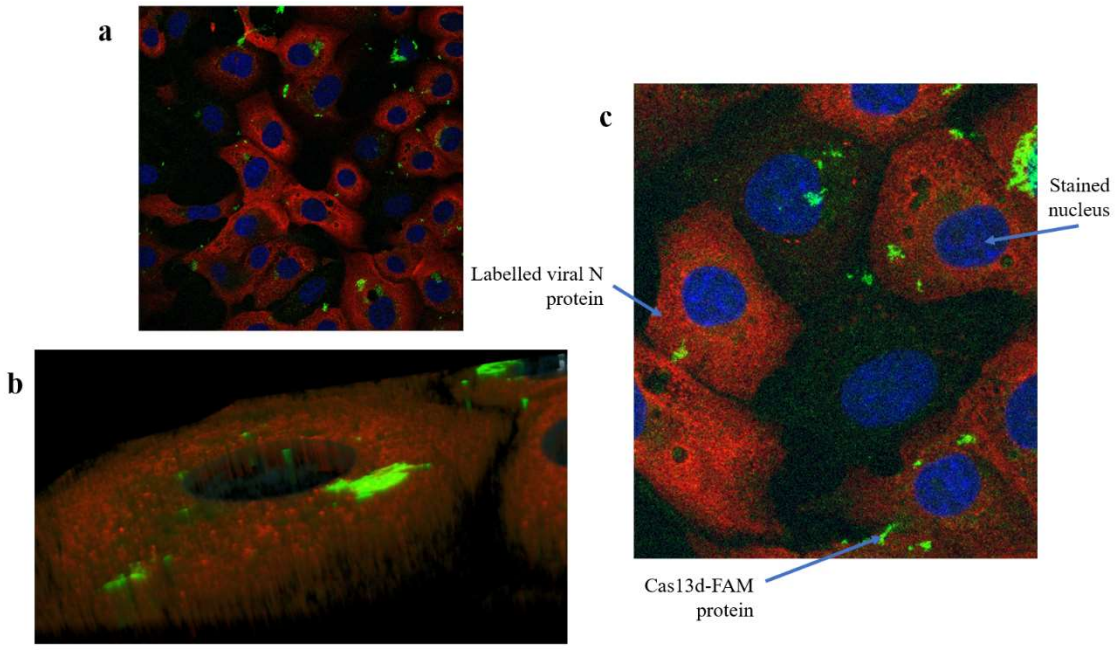

FIGURE 11 | Individual cell level study *via* Confocal light microscopy imaging on labelled molecules of SARS-CoV-2 cellular infection treated with Cas13d RNPs. **(a)** 2D projection of all the section showing uniform distribution of viral N protein (red) and the Cas13d protein (green) aggregates. **(b)** 3D model of an individual cell suggesting the deformation of plasma membrane by protein aggregates. **(c)** Two central healthy cells showing a uniform distribution of Cas13d enzyme surrounded by virus-infected cells.

5. CONCLUSIONS

CRISPR-Cas13d has emerged has a new variant among CRISPR-Cas toolkits. Having a platform to interfere with the expression and activity of RNA with better yields than the technologies previously described, RNAi and MOs, will make it easier to study cell function and pathologies. In this project we assessed the use of the disruptive CRISPR-Cas13d technology as an antiviral drug for the destruction of the RNA genome of viruses in infected cell cultures, with an analogous similarity of the original applications associated with the CRISPR-Cas systems in prokaryotes. One of the main barriers to test this hypothesis is to establish the method to deliver RNPs to the infected cells. Additionally, due to CRISPR-Cas13d system plasticity, its crRNA sequences could be adapted to SARS-CoV-2 variants or new virus which could arise in the future, further highlighting its pan-coronavirus characteristic.

We have characterized the *in vitro* RNase activity of Cas13d effector protein, targeting it against the viral mRNA coding for the N protein of the BEV equine torovirus. We have demonstrated that the biochemically context where Cas13d plus a specific gRNA act also determines the general CRISPR-Cas13d performance; digestion efficiency of the RNPs were different in zebrafish embryos *in vivo* than in purely *in vitro* context. RNPs *in vivo* validations methods are usually considered better when they are studied to be used in therapeutic approaches. However, crRNAs validated in fish cells should be also validated in mammalian cells, whose

cellular contexts might be different. Finally, we reported a moderate *in vitro* collateral activity of *Rfx*Cas13d effector protein.

Here, we showed that electroporation was not an optimal delivery method of CRISPR-Cas13d reagents because it is too toxic for cell viability and results in a low protein introduction ratio. The electroporation of Cas13d effector protein apparently resulted in protein aggregations located outside the cellular membrane. Therefore, it would appear that only few active forms of the Cas13d nuclease were introduced into the cells, thus resulting in a poorly significant genetic interference of SARS-CoV-2 viral infection on cell population. Although, a statistically significant decrease was found in virus titre after Cas13d RNP treatment, this reduction in virus production is promising but not optimal, suggesting that CRISPR-Cas13d could have interfered in SARS-CoV-2 replication. But this trend could have not been confirmed by the analysis of viral protein accumulation in cells nor by the microscopic analysis. Finally, possible toxic effect of Cas13d protein presence in cell should be further assessed. Our main hypothesis could not be verified for the time being.

Transfecting the successfully cloned mammalian expression plasmids carrying the CRISPR-Cas13d reagents, or their IVT RNA products, became a seemingly better alternative for delivering these tools to subsequently test the efficacy of antiviral approach proposed in the present study. Besides, the incubation times required for the optimal expression of the encoding sequences (DNA or RNA) of these reagents have been determined in this study.

The next step could be a proof-of-concept experiment on HcoV-229E virus-infected Huh7 cells cultures using DNA vectors or mRNAs encoding the CRISPR-Cas13d reagents transfected with lipofectamine as a delivery method.

5.1 Limitations and Future Directions

The main bottleneck to test the Cas13d antiviral drug approach is the development of effective and safe *in vitro* cells delivery methods, which would have to be clinically compatible with the eventual treatment of COVID-19 patients. Protein-based liposomal delivery strategies, which are derived from the receptor cells are in development as promising solutions. As soon as this technology is ready, next step would be carrying on a proof-of-concept experiment on BEV equine torovirus, whose gRNAs showed the highest depletion scores (figure 3, a), infecting MRC-5 o E. derm cells in culture. Unfortunately, to date, no reliable delivery method is available for these cell lines (figure 9).

More efforts should be invested to develop more effective gRNAs against conserved regions of the viral genome. Especially for the *RdRp* gene (figure 3). This gene is not found in the sgRNA that are transcribed from the main genome, and since it is only found in viral genomes

and it is essential (figure 1), destroying it could mean a greater genetic intervention in the viability of the virus cycle. Furthermore, on the top of an optimally-designed crRNA, the recently-described chemical modifications could improve their stability throughout the cell cytoplasm (Méndez-Mancilla et al., 2021). Consequently, more persistent and robust RNA viruses knock down could be potentially observed.

This study should progress step by step. At first, ideally, the hypothesis should be studied in HcoV-229E and BEV viruses because their gRNAs were reported with higher depletions score and they can be manipulated under less restrictive manipulation conditions. In these experimental systems we could test and validate several delivery methods, until achieving a really robust, highly efficient, specific and simple system. Thereafter, the optimal conditions could be transferred to the real planned experiment, directly targeting SARS-CoV-2 infected cells.

REFERENCES

Abbott, T. R., Dhamdhere, G., Liu, Y., Lin, X., Goudy, L., Zeng, L., Chemparathy, A., Chmura, S., Heaton, N. S., Debs, R., Pande, T., Endy, D., La Russa, M. F., Lewis, D. B., & Qi, L. S. (2020). Development of CRISPR as an Antiviral Strategy to Combat SARS-CoV-2 and Influenza. *Cell*, *181*(4), 865-876.e12. https://doi.org/10.1016/j.cell.2020.04.020

Abudayyeh, O. O., Gootenberg, J. S., Essletzbichler, P., Han, S., Joung, J., Belanto, J. J., Verdine, V., Cox, D. B. T., Kellner, M. J., Regev, A., Lander, E. S., Voytas, D. F., Ting, A. Y., & Zhang, F. (2017). RNA targeting with CRISPR-Cas13. *Nature*, *550*(7675), 280–284. https://doi.org/10.1038/nature24049

Baraniuk, C. (2021). Where are we with drug treatments for covid-19? Where are the major trials for covid treatments? *The BMJ*. https://doi.org/10.1136/bmj.n1109

Blanchard, E. L., Vanover, D., Bawage, S. S., Tiwari, P. M., Rotolo, L., Beyersdorf, J., Peck, H. E., Bruno, N. C., Hincapie, R., Michel, F., Murray, J., Sadhwani, H., Vanderheyden, B., Finn, M. G., Brinton, M. A., Lafontaine, E. R., Hogan, R. J., Zurla, C., & Santangelo, P. J. (2021). Treatment of influenza and SARS-CoV-2 infections via mRNA-encoded Cas13a in rodents. *Nature Biotechnology*. https://doi.org/10.1038/s41587-021-00822-w

Broughton, J. P., Deng, X., Yu, G., Fasching, C. L., Servellita, V., Singh, J., Miao, X., Streithorst, J. A., Granados, A., Sotomayor-gonzalez, A., Zorn, K., Gopez, A., Hsu, E., Gu, W., Miller, S., Pan, C., Guevara, H., Wadford, D. A., Chen, J. S., & Chiu, C. Y. (2019). *CRISPR – Cas12-based detection of SARS-CoV-2*.

Buchman, A., Brogan, D. J., Sun, R., Yang, T., Hsu, P., Hsu, P., Akbari, O. S., & Akbari, O. S. (2020). Programmable RNA Targeting Using CasRx in Flies. *CRISPR Journal*, *3*(3), 164–176. https://doi.org/10.1089/crispr.2020.0018

Corman, V. M., Muth, D., Niemeyer, D., & Drosten, C. (2018). Hosts and Sources of Endemic Human Coronaviruses. In *Advances in Virus Research* (Vol. 100, pp. 163–188). Academic Press Inc. https://doi.org/10.1016/bs.aivir.2018.01.001

Ding, X., Yin, K., Li, Z., Lalla, R. V., Ballesteros, E., Sfeir, M. M., & Liu, C. (2020). Ultrasensitive and visual detection of SARS-CoV-2 using all-in-one dual CRISPR-Cas12a assay. *Nature Communications*, *11*(1), 1–10. https://doi.org/10.1038/s41467-020-18575-6

Doudna, J. A., & Charpentier, E. (2014). The new frontier of genome engineering with CRISPR-Cas9. *Science*, *346*(6213), 1–10. https://doi.org/10.1126/science.1258096

Engler, C., & Marillonnet, S. (2011). Chapter 11 Using Golden Gate Shuffling. *Springer Science*,

729, 167–181. https://doi.org/10.1007/978-1-61779-065-2

Fernández, A., Hayashi, M., Garrido, G., Montero, A., Guardia, A., Suzuki, T., & Montoliu, L. (2021). Genetics of non-syndromic and syndromic oculocutaneous albinism in human and mouse. *Pigment Cell & Melanoma Research*, pcmr.12982. https://doi.org/10.1111/pcmr.12982

Fernández, A., Josa, S., & Montoliu, L. (2017). A history of genome editing in mammals. *Mammalian Genome*, *28*(7–8), 237–246. https://doi.org/10.1007/s00335-017-9699-2

Harms, D. W., Quadros, R. M., Seruggia, D., Ohtsuka, M., Takahashi, G., Montoliu, L., & Gurumurthy, C. B. (2014). Mouse genome editing using the CRISPR/Cas system. *Current Protocols in Human Genetics*, *83*, 15.7.1-15.7.27. https://doi.org/10.1002/0471142905.hg1507s83

Hille, F., Richter, H., Wong, S. P., Bratovič, M., Ressel, S., & Charpentier, E. (2018). The Biology of CRISPR-Cas: Backward and Forward. *Cell*, *172*(6), 1239–1259. https://doi.org/10.1016/j.cell.2017.11.032

Joung, J., Ladha, A., Saito, M., Segel, M., Bruneau, R., Huang, M. L. W., Kim, N. G., Yu, X., Li, J., Walker, B. D., Greninger, A. L., Jerome, K. R., Gootenberg, J. S., Abudayyeh, O. O., & Zhang, F. (2020). Point-of-care testing for COVID-19 using SHERLOCK diagnostics. *MedRxiv*. https://doi.org/10.1101/2020.05.04.20091231

Kellner, M. J., Koob, J. G., Gootenberg, J. S., Abudayyeh, O. O., & Zhang, F. (2019). SHERLOCK: nucleic acid detection with CRISPR nucleases. *Nature Protocols*, *14*(10), 2986–3012. https://doi.org/10.1038/s41596-019-0210-2

Khodavirdipour, A., Piri, M., Jabbari, S., & Khalaj-kondori, M. (2021). Potential of CRISPR/Cas13 System in Treatment and Diagnosis of COVID-19. *Global Medical Genetics*, *08*(01), 007–010. https://doi.org/10.1055/s-0041-1723086

Kim, D., Lee, J. Y., Yang, J. S., Kim, J. W., Kim, V. N., & Chang, H. (2020). The Architecture of SARS-CoV-2 Transcriptome. *Cell*, *181*(4), 914-921.e10. https://doi.org/10.1016/j.cell.2020.04.011

Konermann, S., Lotfy, P., Brideau, N. J., Oki, J., Shokhirev, M. N., & Hsu, P. D. (2018). Transcriptome Engineering with RNA-Targeting Type VI-D CRISPR Effectors. *Cell*, *173*(3), 665-676.e14. https://doi.org/10.1016/j.cell.2018.02.033

Kushawah, G., Abugattas-Nuñez del Prado, J., Martinez-Morales, J. R., DeVore, M., Guelfo, J. R., Brannan, E. O., Wang, W., Corbin, T. J., Moran, A. M., Alvarado, A. S., Málaga-Trillo, E., Takacs, C. M., Bazzini, A. A., & Moreno-Mateos, M. A. (2020). CRISPR-Cas13d

induces efficient mRNA knock-down in animal embryos. *BioRxiv*. https://doi.org/10.1101/2020.01.13.904763

Lander, E. S. (2016). The Heroes of CRISPR. In *Cell* (Vol. 164, Issues 1–2, pp. 18–28). Cell Press. https://doi.org/10.1016/j.cell.2015.12.041

Méndez-Mancilla, A., Wessels, H.-H., Legut, M., Kadina, A., Mabuchi, M., Walker, J., Robb, G. B., Holden, K., & Sanjana, N. E. (2021). Chemically modified guide RNAs enhance CRISPR-Cas13 knockdown in human cells. *BioRxiv*, 2021.05.12.443920. https://doi.org/10.1101/2021.05.12.443920

Mojica, F. J. M., & Montoliu, L. (2016). On the Origin of CRISPR-Cas Technology: From Prokaryotes to Mammals. In *Trends in Microbiology* (Vol. 24, Issue 10, pp. 811–820). Elsevier Ltd. https://doi.org/10.1016/j.tim.2016.06.005

Nguyen, T. M., Zhang, Y., & Pandolfi, P. P. (2020). Virus against virus: a potential treatment for 2019-nCov (SARS-CoV-2) and other RNA viruses. In *Cell Research* (Vol. 30, Issue 3, pp. 189–190). Springer Nature. https://doi.org/10.1038/s41422-020-0290-0

Nuñez, J. K., Chen, J., Pommier, G. C., Cogan, J. Z., Replogle, J. M., Adriaens, C., Ramadoss, G. N., Shi, Q., Hung, K. L., Samelson, A. J., Pogson, A. N., Kim, J. Y. S., Chung, A., Leonetti, M. D., Chang, H. Y., Kampmann, M., Bernstein, B. E., Hovestadt, V., Gilbert, L. A., & Weissman, J. S. (2021). Genome-wide programmable transcriptional memory by CRISPR-based epigenome editing. *Cell*, *184*(9), 2503-2519.e17. https://doi.org/10.1016/j.cell.2021.03.025

Piergentili, R., Del Rio, A., Signore, F., Umani Ronchi, F., Marinelli, E., & Zaami, S. (2021). CRISPR-Cas and Its Wide-Ranging Applications: From Human Genome Editing to Environmental Implications, Technical Limitations, Hazards and Bioethical Issues. *Cells*, *10*(5), 969. https://doi.org/10.3390/cells10050969

Seruggia, D., Fernández, A., Cantero, M., Pelczar, P., & Montoliu, L. (2015). Functional validation of mouse tyrosinase non-coding regulatory DNA elements by CRISPR-Cas9-mediated mutagenesis. *Nucleic Acids Research*, *43*(10), 4855–4867. https://doi.org/10.1093/nar/gkv375

Seruggia, D., Josa, S., Fernández, A., & Montoliu, L. (2020). The structure and function of the mouse tyrosinase locus. In *Pigment Cell and Melanoma Research* (Vol. 34, Issue 2). Blackwell Publishing Ltd. https://doi.org/10.1111/pcmr.12942

Singh, D., & Yi, S. V. (2021). On the origin and evolution of SARS-CoV-2. *Experimental & Molecular Medicine*, 1. https://doi.org/10.1038/s12276-021-00604-z

Singsuksawat, E., Onnome, S., Posiri, P., Suphatrakul, A., Srisuk, N., Nantachokchawapan, R., Praneechit, H., Sae-kow, C., Chidpratum, P., Hongeng, S., Avirutnan, P., Duangjinda, T., & Siridechadilok, B. (2021). Potent programmable antiviral against dengue virus in primary human cells by Cas13b RNP with short spacer and delivery by virus-like particle. *Molecular Therapy - Methods & Clinical Development*. https://doi.org/10.1016/j.omtm.2021.04.014

Tong, B., Dong, H., Cui, Y., Jiang, P., Jin, Z., & Zhang, D. (2021). The Versatile Type V CRISPR Effectors and Their Application Prospects. *Frontiers in Cell and Developmental Biology* (Vol. 8, p. 622103). Frontiers Media S.A. https://doi.org/10.3389/fcell.2020.622103

Ujike, M., & Taguchi, F. (2021). Recent Progress in Torovirus Molecular Biology. In *Viruses* (Vol. 13, Issue 3). NLM (Medline). https://doi.org/10.3390/v13030435

Yan, W. X., Chong, S., Zhang, H., Makarova, K. S., Eugene, V., Cheng, D. R., & Scott, D. A. (2019). Cas13d is a compact RNA-targeting type VI CRISPR effector positively modulated by a WYL domain-containing accessory protein. *Mol Cell 70*(2), 327–339. https://doi.org/10.1016/j.molcel.2018.02.028.Cas13d

Zhang, F., Chase-Topping, M., Guo, C. G., van Bunnik, B. A. D., Brierley, L., & Woolhouse, M. E. J. (2020). Global discovery of human-infective RNA viruses: A modelling analysis. *PLoS Pathogens*, *16*(11). https://doi.org/10.1371/journal.ppat.1009079

SELF-ASSESSMENT

These 5-month period in the laboratory of Dr. Lluís Montoliu has been a very good experience. Thanks to this internship, I was able to completely integrate in a research group with such an important focus of research field, which is the CRISPR-Cas systems applications and limitations on the study of mammalian genome organization and the generation of transgenic animals models. I applied for the bachelor's degree in Biotechnology, four years ago, for its implication in the genetics field. Biotechnology and genetics are a source of opportunities for our lives, for example through obtaining resources in a more respectful way with the environment, the fight against climate change or the study of human pathologies. Studying the use of CRISPR-Cas13d in limiting the SARS-CoV-2 replication in cells has allowed me to reaffirm that I did well in choosing biotechnology, as the project fits perfectly into its definition. Therefore, it has been a pleasure contributing to the fight against this globally harmful pandemic.

The facilities of the CNB-CSIC are a magnificent environment for personal and professional development. Having participated in this project has helped me to learn how to work in a multidisciplinary team made up of teams located in different locations in the territory: I had the opportunity of working with virus, bioinformatics, flow cytometry and genetics experts, thereby I learnt from different science fields. Living in Madrid has also been a rewarding experience. I started in February with shortcomings in basic laboratory procedures, for example, loading the sample into gel electrophoresis. But now, I have improved my time management and writing skills, becoming completely independent in the experimental work. I have been able to see the experimental part of so many techniques explained during academic lessons, such as, Advanced Confocal Light Microscopy, recombinant DNA technology, eukaryotic cell cultures maintenance and CRISPR-Cas9. Not only I strictly learnt about the CRISPR-Cas13d project.

I would like to specifically thank Almudena Fernández, a great geneticist, for her patience in my supervision. She never lost her temper and has repeated to me everything that I did not understand. Also, to Lucía, with whom I collaborated to do the experiments.

I was hoping to learn about CRISPR-Cas systems applications and ended up learning a lot more. My intention during the writing of this project was to practice my scientific writing skills, making a simile in the style of the scientific articles consulted. I hope this experience is just the beginning of my scientific career in the field of applied genetics.

Thanks for reading my Final Degree Project,

Pau Cunillera Bori

ANNEX

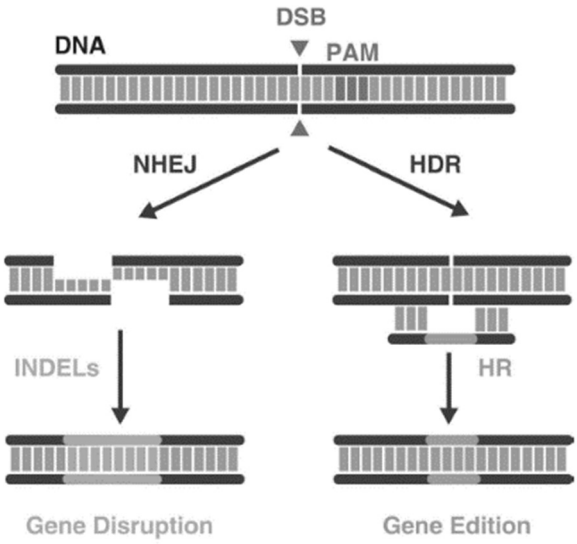

Supplementary figure 1 | A basic diagram depicting the nuclease-mediated genome editing process. This scheme is applicable to all recognized genome editors. The associated nucleases cause DNA cleavage at unique genomic locations, resulting in a double-strand break (DSB) that can be repaired using either of two methods: NHEJ or HDR, as shown. For the most popular CRISPR-Cas9 method used for genome editing, the PAM sequence is necessary. INDELs insertion and deletions, DSB double-strand break, NHEJ non homologous end joining, HDR homology guided repair, PAM protospacer adjacent motif, HR homologous recombination (Fernández et al., 2017).

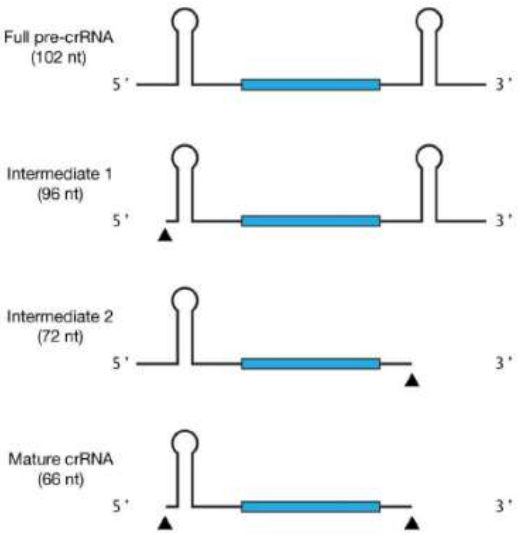

Supplementary figure 2 | Schematic representation of the major products identified from next-generation sequencing of *in vitro* cleaved RNA fragments from the pre-crRNA. (Yan et al., 2019).

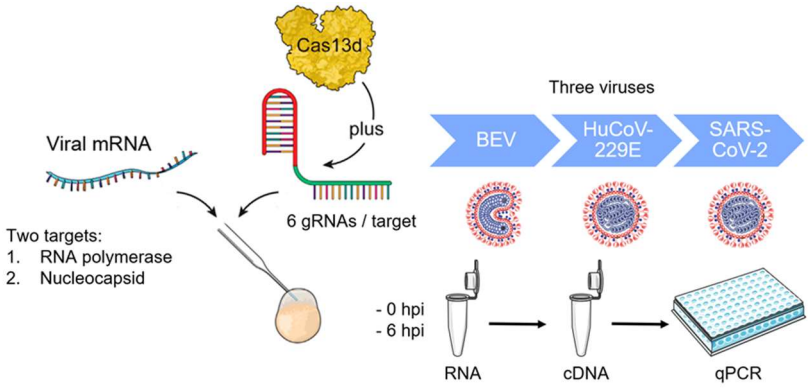

Supplementary figure 3 | Schematic diagram of experimental crRNA validation method based on micro-injection of synthetic viral mRNA and CRISPR reagents into fish embryo and, subsequently, a RT-PCR to assess the dynamics of viral mRNA copies at 6 hpi. The diagram has been generated by Ismael Moreno from Moreno-Mateo's laboratory at CABD in Sevilla.

Text name	Sequence (5'-...-3')
BEV_N_gRNA6	TTAAGCATAGAATTCATTCCCAT
BEV_N_gRNA7	TGGCGCCTATTAAACTGATTACG
BEV_N_gRNA2	ACCAGAAGAAAAACCAGATGGGT
BEV_N_gRNA3	GTGCCATTAGATATCTCTACGGT
SARS-CoV-2_N_gRNA3	CAAGGCTCCCTCAGTTGCAACCC
SARS-CoV-2_N_gRNA4	GTTCCTTGAGGAAGTTGTAGCAC
Fw Cas13d primer (for cloning)	TCTGCAGATATCCATCACACTGGCGGCCGCgccaccatggcgagcgaggccagcatcgaaaaaaaaaagtc
Rv Cas13d primer (for cloning)	ACTATAGAATAGGGCCCTCTAGATGCATGCttaagcgtaatctggaacatcgtatgggtaagcgg
Fw LKO primer	GACTATCATATGCTTACCGT
Rv BEV_N_gRNA6 primer	aaaaagATGGGAATGAATTCTATGCTTAAcc
Rv BEV_N_gRNA7 primer	aaaaagCGTAATCAGTTTAATAGGCGCCAcc
Fw T7 primer	TAATACGACTCACTATAGGG
Rv Cas13d primer	CTGAATTTGGCGTTGCCGAT

Supplementary table 1 | Primers and oligonucleotides sequences used in the present study.

ANNEX 2

FITXA DE SEGUIMENT DEL TUTOR/A del TFG

Nom i Cognoms de l'Alumne/a:__ **Pau Cunillera Bori**

Nom i Cognoms del Tutor/a:___Ximena Terra Barbadora

Data de la entrevista amb l'alumne:___En diverses ocasions per e-mail

Recomanacions durant el seguiment:____Recomanacions sobre l'extensió de la memòria i sobre la revisió de la Normativa TFG penjada a Moodle, recomanacions sobre el contingut de la introducció, recomanacions sobre el contingut dels resultats.

Observacions:____Totes les suggerències han estat correctament rebudes per l'alumne. _____

_____

_____

Observacions Darrera revisió:

_____

Encara no s'ha revisat la darrera versió de la memòria.

_____

_____

_____

_____

Signatura del Tutor/a

Ximena Terra Barbadora

Firmado digitalmente por Ximena Terra Barbadora
Nombre de reconocimiento (DN): cn=Ximena Terra Barbadora, o=Universitat Rovira i Virgili, ou=URV, email=ximena.terra@urv.cat, c=ES
Fecha: 2021.05.24 11:46:48 +02'00'

Signatura del Alumne/a

Pau Cunillera Bori

Firmado digitalmente por Pau Cunillera Bori
Fecha: 2021.05.23 15:34:51 +02'00'

Tarragona a _19_____de __Maig_____20_21__